Journal of Building Engineering 88 (2024) 109175

Contents lists available at ScienceDirect

Journal of Building Engineering

journal homepage: www.elsevier.com/locate/jobe

High-strength self-compacting concrete produced with recycled clay brick powders: Rheological, mechanical and microstructural properties

Ahmet Ferdi Şenol *, Cenk Karakurt

Bilecik Seyh Edebali University, Faculty of Engineering, Department of Civil Engineering, TR, 11100, Bilecik, Turkiye

ARTICLE INFO

Keywords:
High strength self compacting concrete
Fly ash
Recycled clay brick powders
Fresh concrete properties
Mechanical properties
Micro-structurel analysis

ABSTRACT

High-strength self-compacting concrete (HSSCC), which has superior workability and filling ability compared to conventional concrete, is increasingly used in modern densely reinforced structures in the construction industry. However, HSSCC is more costly to produce than conventional concrete and can result in higher carbon emissions due to higher cement usage. On 6 February 2023, the devastating Kahramanmaraş earthquakes in Türkiye created a serious environmental problem. In this context, recycling and utilizing construction demolition waste (CDW), which creates a serious environmental problem after devastating earthquakes and urban transformations, can contribute to the economy of countries and environmental waste problems. In this study, to produce HSSCC more economically, sustainably, and environmentally, HSSCC series were produced using fly ash (FA) and recycled clay brick powders (RCBP) obtained from CDWs in certain proportions by weight instead of cement. For this purpose, seven different series of HSSCC were produced. FA and RCBP were used separately in the mixtures at 0% (control), 10%, 15%, and 20% by weight instead of cement. The fresh HSSCC series were then subjected to workability tests and cured for 28, 56, and 90 days. At the end of the curing period, physical and mechanical property tests and internal structure analyses by scanning electron microscopy (SEM) were performed on the HSSCC series. In addition, sensitivity analysis was performed using multiple linear model analysis to determine which parameters affect which properties in HSSCC designs. Although the highest workability loss in fresh HSSCCs was in the blend series where 20% RCBP was used, all of the blends provided fresh SCC properties by the standards. In general, the increase in FA and RCBP used in the HSSCC series decreased the 28-day compressive strengths (except RCBP10), while the strength losses gradually decreased as the curing age increased and at the end of 90 days; the compressive strengths of FA10 (71.9 MPa with 1.6% increase), RCBP10 (74.8 MPa with 5.6% increase) and RCBP15 (71.5 MPa with 1% increase) series were obtained above the control series (70.8 MPa). SEM analyses performed at the end of the study showed that HSSCC specimens with 10% RCBP replacement contained more intense hydration products and fewer pores than the other series.

1. Introduction

In the developing construction industry, high-rise and long-span modern reinforced concrete structures can be produced with

* Corresponding author.
E-mail address: ahmetferdi.senol@bilecik.edu.tr (A.F. Şenol).

https://doi.org/10.1016/j.jobe.2024.109175
Received 6 December 2023; Received in revised form 8 March 2024; Accepted 28 March 2024
Available online 31 March 2024

densely reinforced and complex geometry structural elements. It can be difficult to place and compact conventional concrete homogeneously in the molds designed to produce these structures and to expect high performance. In case of insufficient compaction, voids may form in the concrete and mechanical strength may decrease as a result. Most of these difficulties can be overcome using self-compacting concrete (SCC) [1]. Starting with the first production studies in Japan in the 1980s [2] SCC is an innovative type of concrete that can be placed in the mold under its weight uniformly and without vibration, generally has higher performance than conventional concrete, and increases the degree of freedom of structural design [3,4]. Unlike conventional vibrated concrete, SCC can shorten the construction period in most reinforced concrete projects by eliminating concerns about noise and compaction [5]. The mixing design of SCC should be easy to apply, durable, conform to technical requirements and strengths, sustainable and cost-effective. In addition, SCCs should have high filling ability, high passing ability, high segregation resistance, and the required mechanical and durability properties [6,7]. A well-designed SCC has fundamental differences compared to conventional concrete. These are less coarse aggregate content, increased paste content, low water/powder ratio and superplasticizers with improved performance [8]. In order to produce a homogeneous and cohesive SCC mix, a powder content of 450–600 kg/m^3 is usually used compared to conventional vibrated concrete [9]. Some of this powder content can be replaced by mineral admixtures such as fly ash, ground granulated blast furnace slag, silica fume, etc. [10].

The high amount of cement used in SCCs not only increases production costs but also leads to a high carbon footprint, which has a detrimental effect on the environment [11–14]. In order to reduce the production costs and environmental damages of SCC, cement consumption can be minimized by adding appropriate amounts of supplementary cementitious materials (SCM) instead of cement in SCC mixtures [15]. For this purpose, the use of supplementary cementitious materials (fly ash, blast furnace slag and silica fume, etc.) instead of cement in SCC can contribute to the reduction of environmental pollution and CO_2 emissions and the recycling of waste powder materials in concrete [16,17]. In many SCC studies to date [9,17,18] the use of industrial by-products (fly ash, blast furnace slag, silica fume, etc.) has been aimed at reducing cement-based production costs and to produce more sustainable and high-performance SCCs.

Fly ash (FA), which is used as a cement substitute in SCC production, is a reliable and easily accessible industrial waste product generated after the combustion of coal used in power generation plants [5,17]. FA particles have a smooth and spherical shape and are usually used in the range of 15–25% instead of cement in SCC. The use of FA in SCC can improve the workability of the mixture by reducing the amount of superplasticiser [19,20]. Moreover, using FA can improve the rheological properties of concrete and reduce cracking in concrete as it generates lower heat of hydration [21]. The use of high amounts of FA in SCC can increase the resistance to yielding [7] while decreasing the early-age mechanical strengths [22,23]. Therefore, it is recommended to use FA in concrete mixtures with a relatively high (but not excessive) water/binder ratio or in SCC containing high doses of high-range water reducer admixture [24]. Siddique [21] reported that SCCs meet the fresh property standards by using FA up to 35% instead of cement and that the compressive strength of SCC mixtures decreased with the increase in FA percentage. Sharbaf et al. [25], investigated the abrasion and mechanical performance of SCC mixtures prepared by using natural pozzolan or FA in the range of 0–37.5% instead of cement. They found that the use of both natural pozzolan and FA in the mixtures generally improved the flowability of SCCs and that the increase in FA in the mixture decreased the seven and 28-day compressive strengths due to the late reactivity of pozzolanic materials, while the 90 and 140-day compressive strengths were higher than the control (0%) mixture at almost all replacement levels. Muhammed et al. [26], investigated the rheological and mechanical properties of high strength self-compacting concrete (HSSCC) produced by using FA, ground blast furnace slag or both at a ratio of 0–60% of the total binder in the mix. As a result of the study, they reported that the increase in FA improved the passing ability of HSSCC more than the other mixtures, while the increase in FA caused a continuous decrease in 28-day compressive strengths.

Destructive earthquakes, urban regeneration and the demolition of buildings at the end of their service life generate construction demolition waste (CDW), which is collected indiscriminately on open land, creating environmental problem areas. An increasing amount of CDW is generated each year by the global construction industry. While many countries, including Japan, Germany and the Netherlands, recycle around 80% of CDW [27], recycling rates are very low in Turkey and other developing countries.

The 7.7 and 7.6 (Mw) earthquakes that occurred in Turkiye on 6 February 2023, with epicenters in Pazarcık (Kahramanmaraş/Turkiye) and Elbistan (Kahramanmaraş/Turkiye), respectively, were recorded as the most destructive earthquakes in Turkiye. As a result of the earthquakes, more than 50.000 lives were lost, and structures close to the epicenters of the earthquakes collapsed, resulting in large amounts of CDW. As a result of the earthquakes, 38.330 buildings were demolished, 20.159 buildings were decided to be demolished urgently, and 203.461 buildings were found to be severely damaged so that they could not be retrofitted [28]. As a result of the collapse of a total of 261.950 buildings in a short period of time, the CDWs generated exceeded the annual CDW production amount in Turkiye and created a serious environmental problem. Thus, the reduction and recycling of CDW in the regions most affected by the earthquake has become an important problem that needs to be solved urgently in Turkiye. Most of the CDW (50%) at construction demolition sites in Turkey consists of bricks and tiles, which are fired clay products used in the construction of partition walls and roofing of buildings. In several studies [29–33] it has been found that approximately 50% of CDWs consist of brick and tile residues. It is evaluated that CDWs, which pose a serious problem for the environment, can be recycled like FA and can contribute to the national economy. Efforts to reuse CDWs in the concrete sector are accepted all over the world due to the increasing demand for concrete in countries. Approximately 37% of CDW in Europe is recycled for use as aggregate, primarily to reduce the consumption of natural materials [34]. Shredded clay bricks and tiles from brick and tile production and CDW are readily available waste materials. Recycling different types of CDW materials (roof tiles, hollow brick, and red clay brick) to be used in the concrete sector will require less work. In this context, it is evaluated that different usage areas of recycled clay brick powders (RCBP) that can be obtained from brick and tile wastes can be investigated in the concrete sector, contributing to the environmental waste system and the national economy.

In some studies conducted by researchers, the use of recycled clay bricks (RCBs) as aggregates in concrete is considered less preferred due to the high water absorption and low mechanical strength of clay brick aggregate [35,36]. Therefore, RCBs are generally used in low-strength roads and non-structural construction [37]. The use of RCB as a cement substitute instead of aggregate has attracted more attention from researchers. Some recent studies have evaluated that the use of more than 25% RCBP instead of cement in normal mortar/concrete mixtures generally leads to lower mechanical properties and that the particle size of RCBP affects the mechanical properties of mortar or concrete [38,39]. Zhao et al. [40], evaluated that with increasing grinding time for RCBP, the specific surface area of clay particles and pozzolanic activity increased, but long grinding time also caused agglomeration of RCBP and high energy consumption. When the structure of RCBPs is analyzed; it is found that these powders have pozzolanic material properties similar to SCMs [30,41,42] and the total percentages of SiO_2, Al_2O_3 and Fe_2O_3 in their composition are generally above 70% [43]. Ge et al. [44] investigated the effects of replacing three different particle sizes of brick powders with cement in proportions of 10, 20 and 30% on the fresh and hardened properties of concrete. As a result of the study, they found that brick powder replacement above 10% greatly reduced the amount of slump of fresh concrete, early age strengths decreased with increasing replacement rates, but as the curing age increased, the strength results of brick powder substituted concretes were similar to those of control concrete. Heikal et al. [45], investigated the use of ground clay bricks (GCB) in SCC. They reported that the compressive strength of the concrete decreased with the GCB content in the absence of SCC admixture, while in the presence of SCC admixture, the amount increased up to 28 days due to the formation of C-S-H (calcium silicate hydrate) in the microstructure of the concrete in a more dense order. Sun et al. [46], used RCBP in SCC at 1, 2.5, and 5% ratios instead of both cement and FA. When the mechanical properties of the specimens produced as a result of the mixtures were examined, they reported that SCC with 1% RCBP reached the highest compressive strength, and the compressive strengths of SCC containing RCBP at 28 and 56 days were higher than SCC without RCBP. Abdulrazzaq [47], investigated the effect of RCBPs substituted for cement at 5%, 10% and 15% on the fresh and hardened properties of C35 grade SCC. He reported that a 5% replacement of cement resulted in a significant increase in the workability of SCC and in the compressive strength, tensile strength and modulus of elasticity of the hardened concrete and a significant decrease in the properties of the hardened concrete. Irki et al. [48] used recycled brick powder of four different finenesses at 5, 10, 15 and 20% as partial replacement of cement in self-compacting mortar. At the end of the experimental studies, they reported that when the fineness of the brick dust was kept constant, the workability decreased as the replacement ratio increased, and the highest compressive strengths were obtained at a 5% replacement ratio, and the low strengths at an early age were due to the pozzolanic activity of the brick dust. Silva et al. [49], conducted a study on the replacement of clay brick residue up to 50% by volume instead of cement in SCC. As a result of the study, they reported that the compressive and tensile strengths decreased up to 90 days with the increase in the level of clay brick powder replacement, and with the increase in the curing time (180 and 360 days), the series using up to 37.5% clay brick powder reached higher values than the reference mixture. The HSSCC literature is rich with in-depth studies evaluating the additive effects of waste marble dust, silica fume, blast furnace slag and FA [50]. Despite the research on the use of RCBP in conventional concrete, there are very few studies on the use of RCBP as a cement substitute in HSSCC. Furthermore, the effect of different curing times on the mechanical and microstructural properties of HSSCC has not been fully investigate.

The large gap between the supply and demand of traditional SCM popular in the concrete industry necessitates the investigation of recycled powders as an alternative to cement. The aim of this study is to investigate the feasibility of using RCBP, which is obtained by recycling brick and tile wastes in CDWs generated after earthquakes, urban transformations and demolition of buildings that have completed their service life, as a cement substitute in HSSCC. The primary focus is to assess RCBP as a potential alternative to cement in High-Strength SCC and to draw comparisons with the utilization of FA, an industrial waste.

Previous researches have primarily concentrated on the application of RCBP in standard concrete with normal strength. While many researchers have investigated the use of RCBP and FA in concrete, there has been little research on the fresh properties and physical, mechanical, and microstructural development of HSSCCs produced by replacing cement with RCBP in varying proportions and at different curing times. On the other hand, to increase the accuracy of performance prediction methods for HSSCC design, further studies should increase the number of experiments to be performed. This may result in increased costs and additional time. Another novelty of this study is the comparison of the results of the sensitivity analysis of the HSSCC design variables using multiple regression techniques with the experimental results. Thus, this study provides a comprehensive evaluation of HSSCCs with RCBP and FA using both experimental methods and statistical analyses. However, the use of roof tile waste obtained from construction demolitions can be combined with masonry demolition waste (hollow bricks and red clay bricks) to obtain RCBP, allowing for the recycling of more waste materials. For this purpose, HSSCCs were produced by substituting RCBP and FA separately at 10, 15, and 20% ratios instead of cement in the mixture series. In addition to these, a control (C) series in which only cement was used was also produced, and the workability, physical and mechanical properties, and microstructural performances of all series were compared. The study aimed to evaluate the appropriate amount of RCBPs obtained from CDWs for use in HSSCCs, to reduce the environmental problem caused by CDWs, and to produce economical and sustainable HSSCCs.

2. Materials and methods

2.1. Materials

Locally sourced CEM I 42.5 R Portland Cement produced at Vezirhan Cement Factory in accordance with TS EN 197-1 [51], and F-type fly ash (FA) sourced from Biga Thermal Power Plant in Turkiye were used for HSSCC production. The RCBP used in the study was obtained by collecting roof tiles (RT), hollow bricks (HB), and red clay bricks (RCB) from local construction demolition sites undergoing urban renewal in Turkiye. Thus, by recycling different types of CDW materials together, less labor and more waste materials were used. The mortar layers around the collected tiles and bricks were first cleaned and then separated according to material

types (RT, HB and RCB) by crushing them to 0–4 mm in the jaw crusher in the laboratory. Then, equal amounts of each of RT, HB and RCB were taken to form a mixture package of recycled clay bricks and tiles. As a final process, the mixture package was ground in a ball mill in the laboratory at a speed of 60 rpm for 120 min to a powder (RCBP) until it reached a suitable fineness (passing through a 90 μm sieve) to be used as a cement substitute (Fig. 1).

The results of the physical and chemical (X-ray fluorescence) analysis of the powder materials used in HSSCC mixtures are given in Table 1, and the particle size distribution curves (laser granulometry analysis) are given in Fig. 2. As seen in Table 1, the main chemical component of the cement is CaO, while the waste products of FA and RCBP are SiO_2. Moreover, the sum of SiO_2+Al_2O_3+Fe_2O_3 of RT, HB and RCB in Table 1 is above 70%. According to TS 25 [52], the sum of these oxides by weight of at least 70% indicates that these materials meet a property that natural pozzolans should have.

The surface texture and particle shape of FA and RCBP in HSSCC blends were observed using a Zeiss LEO 1430VP scanning electron microscope (SEM). According to SEM analysis (Fig. 3); FA was completely spherical and consisted of particles with different sizes and smooth surfaces, while RCBP was composed of particles with irregular and angular shapes and rough surfaces.

Limestone-based crushed stone sand with a fineness modulus of 2.31 and a maximum particle size of 4 mm and crushed stone aggregates with a sieve size of 4–11.2 mm were used as aggregates in the mixtures. Specific gravities of sand and crushed stone aggregates were 2.60 and 2.67, and water absorption percentages were 1.56 and 0.48, respectively. Sieve analysis was performed on fine and coarse aggregates in accordance with TS EN 933-1 [53], and the granulometry curves are shown in Fig. 4.

In HSSCC productions, 50% crushed stone sand and 50% crushed stone aggregate were used by volume. Sika ViscoCrete Hi-Tech25 (1.06 g/cm^3) based on polycarboxylic ether was used as high range water reducer admixture (HRWRA) to ensure sufficient workability in the mixtures, while city tap water was used for mixing and curing applications.

2.2. Methods

2.2.1. Mix design

While designing HSSCC mixes, typical mass and volume distributions given in EFNARC [7] and TS 802 [54] standards were used so that the 28-day target strength of the control (C) mix was at least 60 MPa. A total of seven series of mixes were prepared in which FA and RCBP were used separately at 10, 15 and 20% by weight instead of the cement used in the control (C) mix. The quantities of materials used in the HSSCC series are given in Table 2.

The binder expression in the mix series consists of cement, FA and RCBP. HSSCC series are named as C, FA10, FA15, FA20, RCBP10, RCBP15 and RCBP20. In the series codes, FA; stands for fly ash, RCBP; stands for recycled-fired clay brick waste powders, and the numbers stand for the percentage of powder substituted for cement by weight. For example, FA10 is the HSSCC series with 10% fly ash. As can be seen from Table 2, 500 kg/m3 powder material was used according to EFNARC [7] criteria to ensure fresh properties in HSSCC production. In addition, the water/binder ratio in all series was selected as 0.38. Since the study aimed to produce HSSCC series with similar workability properties, the amount of HRWRA additive used in the series was not used in a fixed ratio. The amount of HRWRA was used in the range of 1.8–2% of the binder material so as not to cause any segregation in all HSSCC mixtures and to meet the fresh property standards.

HSSCC series were prepared in a pan-type concrete mixer with a mixing capacity of 56 L and a rotation speed of 36 rpm. Firstly, coarse and fine aggregate, then cement and FA or RCBP were placed into the concrete mixer and mixed dry for 2 min. Then, half of the mixing water was added and mixed for 2 min until the entire mixture was homogeneously wet. Finally, the HRWRA and the rest of the mixing water were added and mixed for another 2 min, and fresh concrete tests were performed for each series of mixtures.

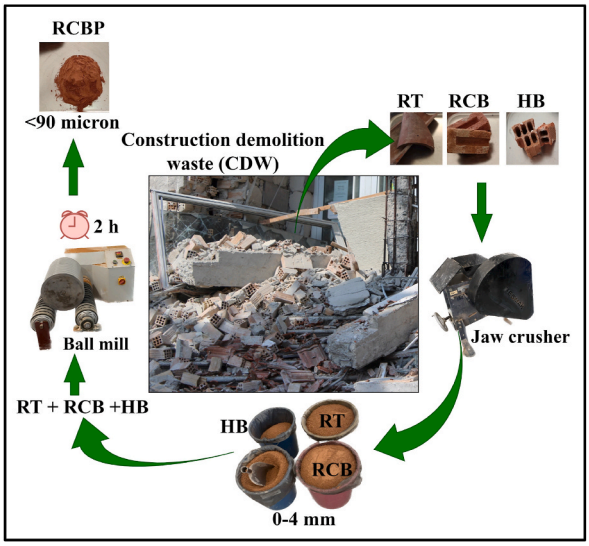

Fig. 1. Stages of preparation of RCBP.

Table 1
Physical and chemical properties of powder materials.

	Oxide Components, %	RCBP			FA	CEM I 42.5 R
		RT	HB	RCB		
Chemical properties (XRF)	SiO_2	44.7	48.9	44.6	52.2	18.7
	Al_2O_3	14.7	17.2	17.2	21.6	4.6
	Fe_2O_3	12.2	7.1	9.8	7.2	3.4
	CaO	8.8	4.7	7.5	8.6	63.7
	MgO	5.2	6.5	6.8	2.3	1.3
	SO_3	0.3	3.5	0.3	1.1	2.7
	K_2O	1.6	3.2	3.2	2.5	0.7
	TiO_2	1.9	0.8	0.8	1.1	–
	P_2O_5	1.3	1.2	1.1	1.1	–
	Mn_2O_3	0.2	0.1	0.1	0.1	–
	Loss of ignition	9.1	6.8	8.6	2.1	3.9
	Free CaO	–	–	–	–	0.8
Physical properties	Specific gravity	2.9	2.9	2.8	2.3	3.1
	Specific surface, m^2/kg	604			304	319
	Initial setting time, min	–			–	195
	Final setting time, min	–			–	260
Compressive strength	2 days, MPa	–			–	25.7
	7 days, MPa	–			–	41.3
	28 days, MPa	–			–	55.8

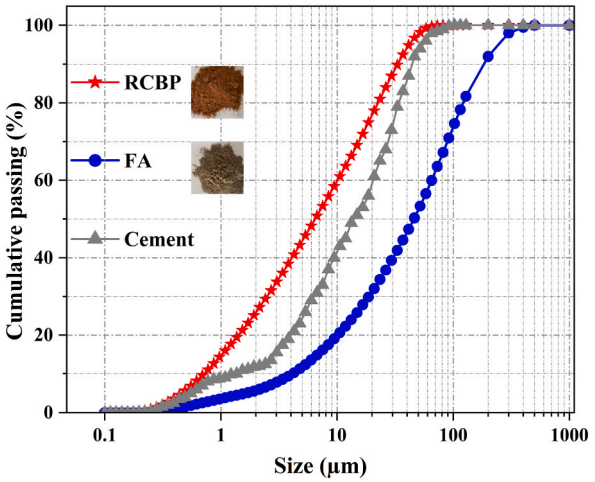

Fig. 2. Particle size distribution curves of powder materials.

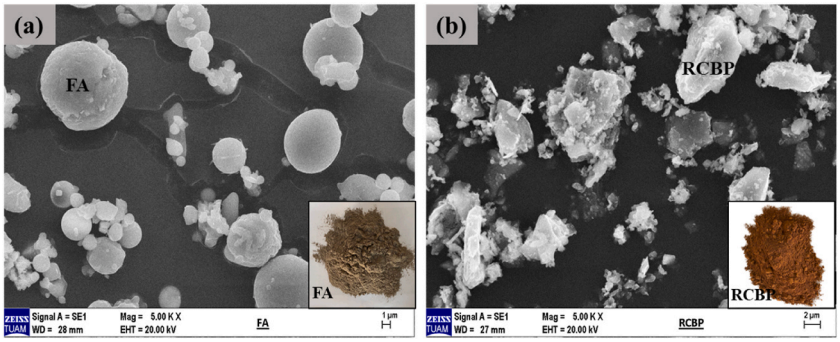

Fig. 3. SEM micrographs (a) FA, (b) RCBP.

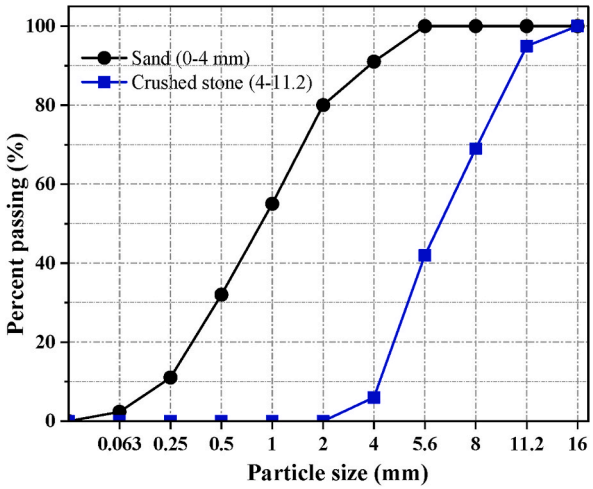

Fig. 4. The granulometry curves of aggregates used.

Table 2
The mixing ratios of the HSSCC series (kg/m^3).

Mixes	Water	Cement	FA	RCBP	Crushed sand (0–4 mm)	Crushed stone (4–11.2 mm)	HRWRA
C	190	500	–	–	829	837	9
FA10	190	450	50	–	821	829	9
FA15	190	425	75	–	817	826	9
FA20	190	400	100	–	814	822	9
RCBP10	190	450	–	50	825	834	10
RCBP15	190	425	–	75	824	833	10
RCBP20	190	400	–	100	823	832	10

2.2.2. *Fresh concrete tests*

In order to determine the fresh properties of HSSCCs, the Slump-flow test and T500 time (time required to reach 500 mm flow diameter) measurement according to TS EN 12350-8 [55], V-funnel test according to TS EN 12350-9 [56] and L-box test with three rebars according to TS EN 12350-10 [57] was applied to the series. The fresh concrete test results of the HSSCC series were also classified according to the target limits (Table 3) specified in the EFNARC [7] guidelines.

2.2.3. *Specimen preparation and curing*

After the fresh concrete tests were performed on the HSSCC series, they were cast into molds. For each series and curing age of the fresh concrete produced, six 100mm × 100mm × 100 mm cube specimens and three 100mm × 100mm × 500 mm beam specimens were poured without vibration. The HSSCC series were kept in the molds in the laboratory environment (20 ± 2 °C) for 24 h and then removed from the molds. The demolded HSSCC specimens were subjected to standard curing in a lime-saturated water pool at 20 ± 2 °C for 28, 56 and 90 days and then hardened concrete tests were performed. A total of 126 cube specimens and 42 beam specimens were produced for the study.

2.2.4. *Hardened concrete tests*

In order to determine the mechanical properties of the HSSCC series, hardened concrete tests were performed on specimens

Table 3
Target limits prescribed by EFNARC.

Test name	Class	Acceptable range	
		Min.	Max.
Slump flow (mm)	SF1	550	650
	SF2	660	750
	SF3	760	850
T_{500} (sec)	VS1	≤2	
	VS2	>2	
V-funnel (sec)	VF1	≤8	
	VF2	9–25	
L-box (h_2/h_1)	PA1	≥0.80 with 2 rebars	
	PA2	≥0.80 with 3 rebars	

prepared in accordance with TS EN 12390-1 [58] and TS 12390-2 [59] standards. After 28, 56 and 90 days of standard curing, unit volume weight (dry), apparent porosity and water absorption by weight tests were performed according to TS EN 772-4 [60] and ASTM C642 [61]. Compressive strength tests (Fig. 5a) were performed according to TS EN 12390-3 [62] using a 2000 kN capacity digital universal testing machine at a constant loading rate of 0.6 ± 0.2 MPa/s.

Archimedes balance was used to calculate the unit volume weight, apparent porosity and percent water absorption by weight of the cube specimens. After curing, the samples were dried in an oven for a period of 24 h until they reached a constant weight. After the measurements were made, the oven-dried samples were placed in a water tank with at least 50 mm of water covering them and kept in water for 48 h. Then, their apparent weights in water and their weights in the water-saturated state after they were removed from the water and their surfaces were wiped with a damp cloth were determined. The unit volume weights, apparent porosity and percent water absorption by weight of the HSSCC series were calculated using Equations (1)–(3).

$$\text{Unit weight (UW) (kg/m}^3\text{)} = [W_1/(W_3\text{-}W_2)] \quad (1)$$

$$\text{Apparent porosity (AP) (\%)} = [(W_3\text{-}W_1)/(W_3\text{-}W_2)] \times 100 \quad (2)$$

$$\text{Water absorption (WA) (\%)} = [(W_3\text{-}W_1)/(W_1)] \times 100 \quad (3)$$

In the equations W_1: Invariant dry weight (g) of the specimen after standing in an oven at 105 °C for 24 h, W_2: Suspended weight of the water-saturated specimen in water (g), W_3: Weight of the water-saturated specimen in air (g).

Three-point flexural strength tests after 28 and 90 days of standard curing were performed on beam specimens according to TS EN 12390-5 [63] (Fig. 5b). The loading setup in the flexural strength test is shown in Fig. 5b and 6 consists of one load application cylinder placed in the center of the span. The loading rate was set at 0.05 MPa/s, and the flexural strength (F_{cf}) of the specimens was calculated using Equation (4).

$$F_{cf} = \frac{3\,P\,L}{2\,d_1 d_2^2} \quad (4)$$

F_{cf} in Equation (4): Flexural strength (MPa), P: Maximum load (N), L: Clearance between support cylinders (mm), d_1 and d_2: Cross-sectional dimensions of the specimen (mm).

The internal structure image analysis of the specimens of the HSSCC series after 28 and 90 days of curing was evaluated using a Zeiss LEO 1430VP scanning electron microscope (SEM). In addition, Energy Dispersive X-ray (EDX) analysis was performed together with SEM to evaluate the chemical elements present on the surface of the specimens.

The production process and applied experiments of HSCCC series are shown in the flow chart in Fig. 7.

3. Results and discussion

3.1. Fresh concrete test results

Fresh concrete tests were conducted to determine the flowability, filling and transition ability of the HSSCCs. In most of the studies in the literature, it has been reported that the flowability of SCC was examined by slump flow test, viscosity was evaluated by T_{500} test, and passing ability was measured by L-box [5]. According to the fresh concrete tests, it was determined that no segregation occurred in all of the series, and HSSCC was produced in accordance with the fresh state standards specified in EFNARC [7] guide, TS EN 12350-8 [55], TS EN 12350-9 [56] and TS EN 12350-10 [57].

3.1.1. Slump-flow and T_{500} times outcome analysis

Slump-flow and T_{500} times results of the HSSCC series are given in Fig. 8.

Fig. 8 shows that the slump-flow results of the series vary between 660 and 800 mm and meet EFNARC [7] standards for SCC slump-flow value. As it is known, SCC at a slump-flow of 550 mm may not have enough flow to pass through highly compacted reinforcement, and the flow diameter reaching 850 mm may cause segregation in the concrete. The highest slump-flow value in the

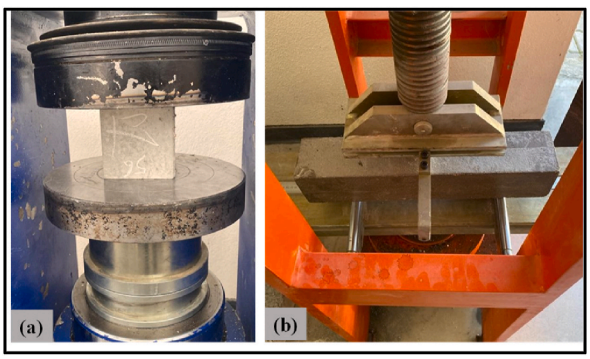

Fig. 5. Mechanical tests (a) Compressive strength, (b) Flexural strength.

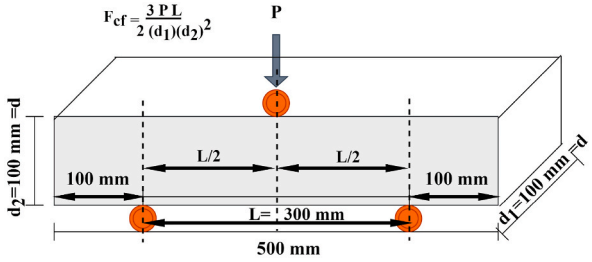

Fig. 6. Beam flexural strength loading setup.

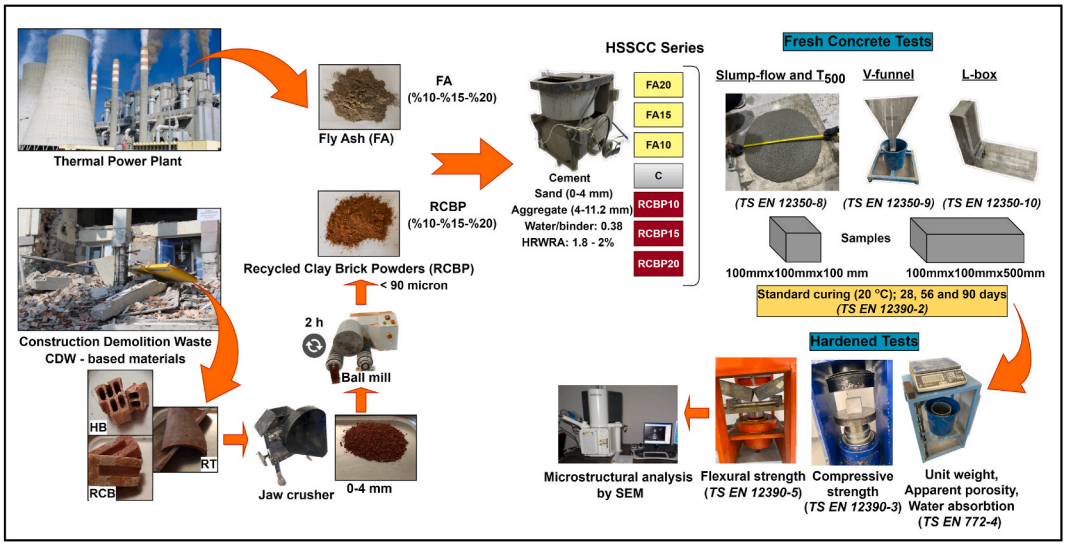

Fig. 7. Flowchart of the mixing and testing procedures.

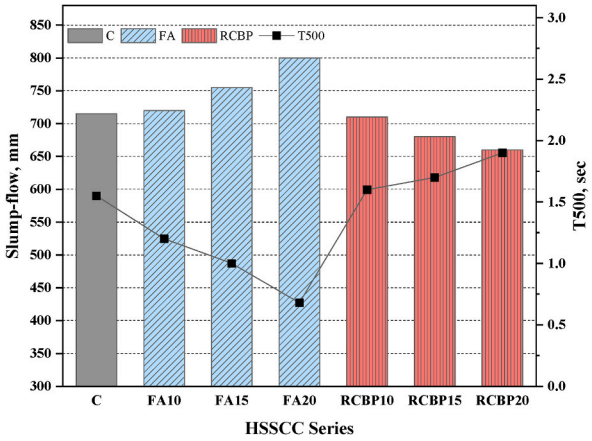

Fig. 8. Slump-flow and T_{500} times measurement results of HSSCC series.

HSSCC series was observed in the FA20 series (800 mm) and the lowest slump-flow value in the RCBP20 series (660 mm). Accordingly, it was determined that FA20 of the HSSCC series is in the SF3 class, and the other series are in the SF2 class. The slump-flow values of the series increased with the increase of FA replacement rate in the mixture compared to series C, while it decreased with the increase of RCBP replacement rate. In addition, after the highest, (at FA20) and lowest (at RCBP20) slump-flow values obtained from the slump-flow tests applied to the HSSCC series, a suitable homogeneity was observed in the concretes (Fig. 9) and no segregation and bleeding tendencies were detected.

The slump-flow values in FA10, FA15 and FA20 series increased by 0.7%, 5.6% and 11.9%, respectively, compared to the C series.

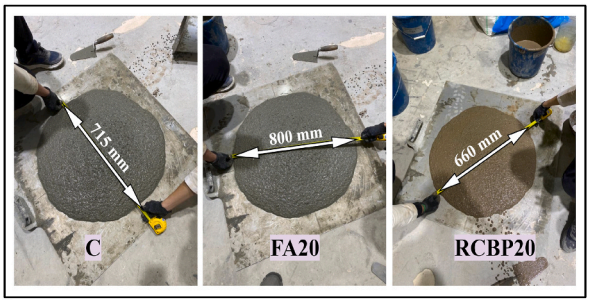

Fig. 9. Slump-flow images of the C, FA20 and RCBP20 series.

As can be seen, increasing the FA content in the HSSCC mixture from 0% to 20% increased the slump-flow value by 11.9%. In a study conducted by Mustapha et al. [64], they reported that the slump-flow values increased by 16.4% when 25% FA was substituted for cement in the high-performance SCC mix compared to the control series. Similarly, Elsayed et al. [65] reported that the slump-flow measurements of SCC mixtures containing 25% and 50% FA replacement increased by 31.4% and 37.3%, respectively, compared to the reference mixture. The fully spherical and smooth-surfaced particles of FA substituted in HSSCC may have caused less internal friction in the mixing paste, making the flow more uniform. This also allows the amount of HRWRA used to be reduced. The increase in workability with increasing FA can also be attributed to the fact that FA in the mix acts as a lubricant, reducing the agglomeration of cement particles due to its spherical shape [66] and reducing the shear force between aggregates and cement paste through the ball bearing effect [64]. In addition, it can be concluded that the increase in the HRWRA effect on the cement, the amount of which decreased compared to the control mix due to FA not reacting with HRWRA, contributed to the increase in workability. Uysal ve Sümer [67] reported in a study that FA, which they used up to 35% by weight instead of cement in SCC, was able to disperse the agglomeration of cement particles due to its spherical shape, using a lower superplasticizer dosage to maintain the same filling ability as cement, and produce higher slump-flow values than cement. The FA replacement used in the study was considered to improve the workability of the HSSCC series and may also contribute to reducing the amount of water or HRWRA to be used in the mix-up to a certain ratio [68].

As the RCBP replacement rate in the HSSCC series increased, slump-flow values in RCBP10, RCBP15 and RCBP20 series decreased by 0.7%, 4.9% and 7.7%, respectively, compared to the C series. Increasing the RCBP content in the HSSCC mix up to 20% decreased the slump-flow values by 7.7% at most. This can be attributed to the fact that RCBP has irregular and angular shapes and rough surface particles in the SEM analysis, as mentioned in Section 2.1. In addition, the fact that the specific surface area of RCBP (604 m^2/kg) is higher than that of cement (314 m^2/kg) with the constant water/binder ratio in the mixture can be considered as the increased water demand reduces the amount of slump-flow. The addition of RCBP to HSSCC mixtures had almost no visible effect (segregation etc.) on the workability of the mixtures. However, the dosage of HRWRA (Table 2) was slightly increased with the increase in the proportion of RCBP in the mixtures in order to prevent detrimental effects on flowability and to meet the SCC fresh criteria (keeping the slump-flow diameter above 550 mm).

According to the T_{500} time results of fresh HSSCCs, all series reached 500 mm diameter in less than 2 s (0.7–1.9 s) (Fig. 8). Therefore, all HSSCC series are classified as VS1 [11]. RCBP20 had the highest T_{500} value, while FA20 had the lowest T_{500} time. The T_{500} time decreased as the FA replacement ratio in the series increased, while the T_{500} time increased as the RCBP replacement ratio increased. It was found that the series with low slump-flow values reached higher T_{500} times, and there was a negative relationship between slump-flow values and T_{500} times. In a study by Schackow et al. [69], it was reported that CBW particles, which are finer than cement in mortars containing generally pulverized baked clay brick waste (CBW), produce less spreading due to increased water

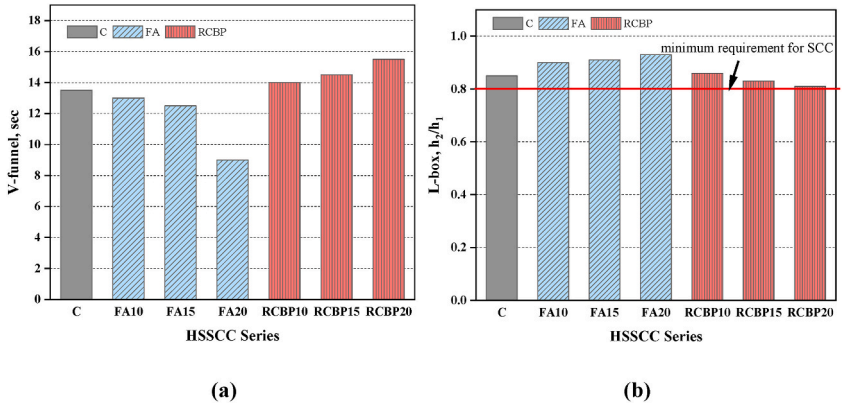

Fig. 10. Workability results of HSSCC series (a) V-funnel, (b) L-box.

consumption and constant water/cement ratio. In a study by Chen et al. [33], they reported that RCBP reduced the workability of cement mortars. They attributed this finding to the fact that RCBP has a larger specific surface area and irregular surface particles than cement, forming pores that increase water absorption more.

3.1.2. Results analysis of V-funnel times and L-box ratios

The V-funnel test applied to the HSSCC series was applied to reveal the filling capacity and viscosity of the mixtures. This test is also an indicator of clogging when unloading times are prolonged [70]. The results of the V-funnel and L-box tests of the HSSCC series are given in Fig. 10.

The V-funnel flow times obtained from the series (Fig. 10a) are between 9 and 15.5 s, which is within the recommended range for SCC. The V-funnel flow values in FA10, FA15 and FA20 series decreased by 3.7%, 7.4% and 33.3%, respectively, compared to series C. As the RCBP replacement rate increased in the HSSCC series, the V-funnel values in the RCBP10, RCBP15 and RCBP20 series increased by 3.7%, 7.4% and 14.8%, respectively, compared to the C series. Since the durations of all series are above 9 s and below the maximum duration limit of 25 s, they are referred to as the VF2 class [11]. In particular, the RCBP-substituted HSSCCs reached durations in the range of 14–15.5 s. Among the series, the FA20 series reached the shortest time (9 s), and the RCBP20 series reached the longest time (15.5 s). The higher value obtained from the V-funnel means lower filling capacity and higher concrete viscosity. The long times obtained during the test can be attributed to the rough surface properties of RCBP and the short times to the spherical particle structure of FA. Similar considerations were also found by other researchers. In a study by Mustapha et al. [64], they substituted 25% FA for cement in SCC and found that the V-funnel flow time improved by 3.3% compared to the control series and measured 11.6 s. It was found that the V-funnel flow times of the series with higher T_{500} times were also higher, and there was a positive correlation between them.

The L-box test results (h_2/h_1 ratios) performed to determine the transition ability characteristics of the HSSCC series ranged from 0.81 to 0.93 (Fig. 10b). According to EFNARC [7] guidelines, the blocking ratio should be between 0.8 and 1.0. All of the fresh HSSCC blends produced were found to meet these requirements. In addition, all series were considered to be of PA2 class [11] and capable of passing through densely reinforced structural elements without blocking. The L-box height ratios in FA10, FA15 and FA20 series increased by 5.9%, 7.1% and 9.4%, respectively, compared to the C series, while in the RCBP series; it increased by 1.2% in the RCBP10 series and decreased by 2.4% and 4.7% in RCBP15 and RCBP20 series. From the results, it is clear that as the amount of RCBP increases, the resistance to yielding also increases, which decreases the passing ability of the concrete. However, the inclusion of FA in the mix improved the L-box height ratio. Accordingly, it was evaluated that FA replacement up to 20% in HSSCC increased the L-box height ratios, while the use of more than 10% RCBP negatively affected the blocking ratio.

3.2. Hardened concrete test results

3.2.1. Unit weight test results

The dry unit volume weights of the HSSCC series after 28, 56 and 90 days of curing are shown in Fig. 11. As expected, the unit volume weights of FA and RCBP substituted HSSCC series decreased compared to the C series.

The 28-day unit volume weights of the HSSCC series ranged between 2451 and 2484 kg/m^3, while the unit volume weights at the end of 90 days ranged between 2456 and 2486 kg/m^3. The 28-day unit volume weights of the samples decreased by 0.7%, 1% and 1.3% in the F10, F15 and F20 series, respectively, while the RCBP10, RCBP15 and RCBP20 series decreased by 0.4%, 0.5% and 0.7%, respectively, compared to the C series. The lower specific gravity of FA and RCBP compared to cement resulted in lower unit weights for the FA and RCBP series compared to the C series. Weight replacement of the materials in the mixtures was also the reason for the decrease in dry density. The decrease in the density of hardened SCC specimens when FA was substituted for cement in SCC mixtures was found in a study by Jain et al. [71]. The lower unit volume weights of the HSSCC series with FA and RCBP replacement may also contribute to the reduction of the dead load of a structure. This may contribute to reducing the cross-sections of structural elements and

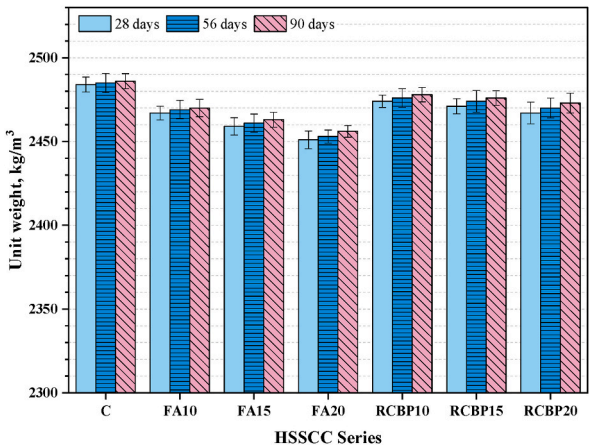

Fig. 11. Unit weight change of HSSCC series according to curing times.

the risk of earthquake damage [72,73]. The unit volume weights of all HSSCC series increased very slightly, about 1%, from 28 days to 90 days of cure. This is considered to be due to the increase in hydration of the series with the increase in curing time and the series becoming more void-free. A similar change was also found in an SCC study by Silva et al. [49] at 28 and 180 days of cure (unit volume weight increase close to 1% with increasing cure time).

3.2.2. Compressive strength test results

The compressive strengths of the HSSCC series after 28, 56 and 90 days of curing are given in Fig. 12. As can be seen in Fig. 12, the compressive strengths of the series increased with increasing curing time. This can be explained by the improvement in hydration reactions.

The 28-day compressive strengths of the HSSCC series ranged between 53.2 and 67.2 MPa, 56-day compressive strengths ranged between 59.5 and 69.8 MPa and 90-day compressive strengths ranged between 63.5 and 74.8 MPa. When the first 28-day compressive strengths of the HSSCC series were analyzed, the compressive strengths of all series except RCBP10 were below the C series. After 28 days of curing, the compressive strengths of FA10, FA15 and FA20 series decreased by 2.3%, 10.4% and 16.2%, respectively, while RCBP10 series increased by 1.5%, RCBP15 and RCBP20 series decreased by 8.2% and 19.6%, respectively. From the 28-day compressive strength results of the series, it is clear that the rate of pozzolanic reaction for FA contributed to the decrease in strength. FA acts as a pozzolan in HSSCC and is, therefore, non-reactive. The compressive strength observed at 28 days of curing was significantly lower, and the compressive strength also improved with the extension of the curing time [74]. The increase in the compressive strengths of RCBP10 at all curing times may be due to the micro-filling ability of RCBP [45] and the formation of better hydration products. The same observation is also observed by internal structure analysis (Section 3.2.7). In various studies [64], it was reported that low CaO content and high SiO_2 and Al_2O_3 content as a result of the reduction of cement in the mixture had a negative effect on the hydration of the binder, resulting in the formation of a smaller amount of CASH gel and a decrease in the early wet compressive strength values of SCCs [75]. When the compressive strengths of the HSSCC series at the end of 56 days of curing were examined, it was found that the differences between the compressive strength of the C series decreased compared to the 28-day results. At the end of 56 days of curing, the compressive strength of the FA10 series increased by 1.3% compared to the C series, while the strengths of the FA15 and FA20 series decreased by 8.5% and 12%, respectively. In the RCBP series, the compressive strength of RCBP10 increased by 1.9%, while the compressive strengths of RCBP15 and RCBP20 series decreased by 2.9% and 13.1%, respectively.

The higher the FA replacement level in HSSCC, the greater the reduction in hardening properties, as a sufficient amount of cement-derived hydration products cannot react with FA [66]. The reduction in compressive strength of Portland cement concrete containing FA may be due to the slow pozzolanic reaction of FA and its dilution effect [64,76]. Since the average particle size of FA is higher than that of cement and RCBP, the pores in the cement paste and interfaces are not completely filled, so the use of FA at 15% and above can also cause a decrease in strength. However, the strength increases in FA10, RCBP10 and RCBP15 series are considered to be due to pozzolanic reactions. The low activity of FA particles in the mixture may have delayed the strength development of HSSCCs up to 56 days (in FA15 and FA20), while the higher fineness of RCBP compared to cement and FA may have increased the strength development due to its pore filling ability and high pozzolanic effect.

In the literature, FA is known to improve the compressive strength of concrete over time. While the replacement of high amounts of FA has a negative effect on the early strength of concrete, it can also reach a remarkable strength at later ages [64]. When the curing period applied to the HSSCC series reached 90 days, it was found that the compressive strength of the FA10 series increased by 1.6% and decreased by 3% and 9.3% in the FA15 and FA20 series compared to the C series. This decrease in compressive strength can be attributed to the increase in class F FA (8.6% CaO), whose CaO content is lower than that of cement (63.7% CaO). The decrease in CaO content due to the decrease in cement with the increase in FA replacement in the mix may have a negative effect on binder hydration [65], resulting in a further decrease in the compressive strength values of HSSCC. When the RCBP series were analyzed, it was found that the 90-day compressive strengths of RCBP10 and RCBP15 series increased by 5.6% and 1%, respectively, while the RCBP20 series

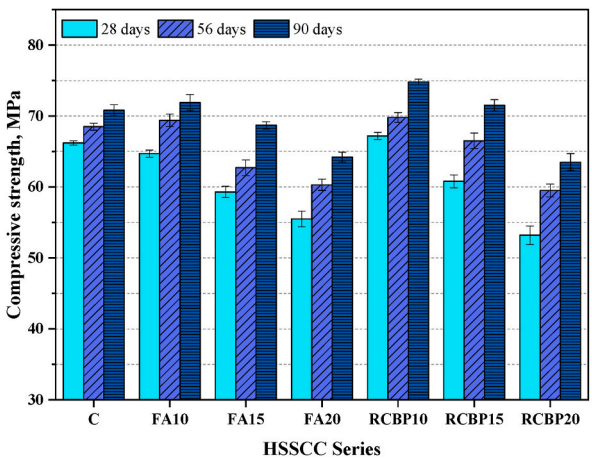

Fig. 12. Compressive strength test results of HSSCC series according to curing times.

decreased by 10.3%. At the end of the 90-day cure applied to the HSSCC series, the RCBP10 series reached the highest compressive strength obtained from all series with a compressive strength value of 74.8 MPa. Since the fineness of pozzolans is an effective factor in accelerating pozzolanic reactions [77], the pozzolanic performance of RCBP used in the mixture at the end of 90 days may be due to its high amount of fineness (604 m^2/kg). In a study conducted by O'Farrel et al. [41], it was found that the early age (up to 28 days) compressive strengths of mortars decreased compared to the control series when cement finely ground brick powders were substituted for cement at 0–30% rates, while the strengths of mortars with low replacement rates (up to 20%) after 90 days of curing were higher than the control series. The fact that the compressive strengths of the FA15, FA20 and RCBP20 series were below the C series strengths at all curing times can be attributed to the decrease in the amount of calcium-silica-hydrate (C-S-H) gels and calcium-hydrate (CH) that provide compressive strength by decreasing the cement content in the mixture. The low bonding between aggregate and paste for this series was also observed by SEM analysis in Section 3.2.6.

In general, the increase in FA and RCBP replacement in HSSCC series decreased the early age compressive strengths, while the strength losses gradually decreased as the curing age increased (56 and 90 days); compressive strengths above series C were obtained in FA10, RCBP10 and RCBP15 series. The strength losses decrease with increasing curing time because the microstructure of the series becomes more compact at the end of the 90-day cure, and additional C-S-H (calcium-silicate-hydrate) gels or C-A-H (calcium aluminate hydrate) are formed. This can be observed from the 28 and 90-day internal structure views of the FA and RCBP replacement HSSCC series in Figs. 24 and 25 of the 3.2.7 Internal Structure Analysis section. Research in the literature indicates that long curing times are required for the dissolution of active Si and Al in RCBP. Additionally, it has been observed that RCBP silicates react with $Ca(OH)_2$, resulting in the production of additional C-S-H gel and an increase in compressive strength at advanced ages due to the thinning of pore structures. According to the results of similar studies [49,70] the use of cement in the concrete mix decreases as the replacement ratio of RCBP and FA increases, the strength of the concrete at the early stage decreases with the increase of the water/cement ratio, but the pozzolanic activities of RCBP and FA become effective with the increase of the curing time. It is evaluated that the compressive strength losses after the 28th day of the series decreased over time as the newly produced gel products filled some pores and strengthened the transition zone between paste and aggregate.

Although the compressive strengths of the RCBP20 series measured up to 90 days were also below series C, it was determined that the difference in compressive strength decreased with the increase in curing time due to the effect of pozzolanic activity. Accordingly, the 28-day compressive strength of RCBP20, which reached the lowest strength among the series, was 80% of series C, while the 90-day compressive strength was 90% of C. Liu [66], in a study using up to 80% FA replacement instead of cement in SCC, reported that the SCC series with FA gained strength close to the control concrete at the end of 90 days of curing and that 20% FA replacement was optimum. Zhang et al. [78], reported in a study that the compressive strength losses obtained from mortar series in which cement was replaced with RCBP at 10, 20 and 30% decreased over time up to 90 days, and the strength loss in the series with 10% RCBP replacement decreased to 0.1%. Similarly, Irki et al. [48], reported that self-compacting mortar specimens produced with up to 15% RCBP replacement reached higher compressive strengths than control mortars at the end of 28 and 90-day curing periods.

3.2.3. Flexural strength test results

The variation of the HSSCC series according to curing times and flexural strengths is given in Fig. 13. As can be seen in Fig. 13, the flexural strengths of the series increased with increasing curing times.

The flexural strengths of the series at the end of 90-day curing varied between 7.9 and 10 MPa. The flexural strength values of series C at the end of 28 and 90 days of curing were 6.3 and 8.6 MPa, respectively. When Fig. 13 is analyzed, the flexural strengths of FA10, FA15 and FA20 series at the end of the 28th day decreased by 3.2%, 4.8% and 11.1%, respectively, compared to series C. In the RCBP series, the strength of RCBP10 increased by 9.5%, while the strength of RCBP15 and RCBP20 series decreased by 3.2% and 11.1%, respectively. Thus, at the end of the first 28 days, the flexural strengths decreased as the FA and RCBP replacement increased in the series except for RCBP10. This improvement in flexural strength of RCBP10 can be attributed to the low porosity and good strength of

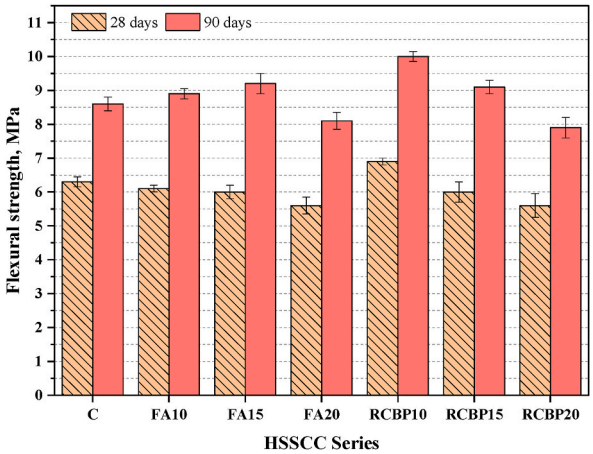

Fig. 13. Flexural strength test results of HSSCC series according to curing times.

both the cement paste matrix and the interfacial transition zone. In addition, the angular shape and rough surface of the RCBP particles provided a tight interlock between the binder and aggregate phase, which may have resulted in increased flexural strength. In the apparent porosity measurements, it was determined that the porosity of RCBP10 was 5.8% lower than the 28-day porosity value of series C. The 28-day flexural strength results of the RCBP series are consistent with the 28-day flexural strength results obtained by Xue et al. [79] from mortar specimens produced with up to 20% RCBP instead of cement. Xue et al. [79] explained that the optimum amount of brick powder (up to 20%) can fill the voids between the cement particles, and brick powder improves the structure of the transition zone between cement paste and aggregate and contributes to flexural strength.

When the flexural strengths of the HSSCC series at the end of the 90-day curing period were analyzed, it was found that the strengths of FA10 and FA15 series increased by 3.5% and 7%, respectively, while FA20 decreased by 5.8%. It is evaluated that the hydration activity of FA-substituted cement decreases due to the decrease in its content in the mixture, resulting in lower flexural strength at early ages (28 days), and when the curing time is extended (90 days), it reaches values above the C series strength due to the continuous improvement of micro-level properties (crack widths, etc.) [80]. This can also be explained by the low calcium content of Class F FA, which slows down the pozzolanic reactions in the concrete and leads to a significant delay in the early strength gain. Similar studies [73,80] found that this effect was more pronounced with higher amounts of FA replacement. In the RCBP series, the 90-day strengths of RCBP10 and RCBP15 increased by 16.3% and 5.8%, respectively, while RCBP20 decreased by 8.1% compared to the C series. In a similar study, Ge et al. [44] evaluated that the higher flexural strengths obtained from concretes produced with RCBP substituted up to 30% instead of cement may be due to a greater bond strength between the rough surface of RCBP and the cement matrix. The flexural strength of the HSSCC series improved after high curing ages (90 days) compared to low curing ages (28 days). As reported in the literature, FA reacts with calcium ions in calcium hydroxide (C-H) to form calcium silicate hydrate (C-S-H), the binder phase. Concretes containing FA do not gain high strength at an early age due to low amounts of C-S-H and C-H [5].

Among the HSSCC series, the 28-day flexural strengths of the series containing 10% and 15% FA and 15% RCBP decreased compared to the C series, as shown in Fig. 13. However, the flexural strengths at the end of the 90-day curing period were higher than those of the C series. The cross-sectional views of the HSSCC series obtained after the flexural strength tests applied to the 90-day beam specimens are shown in Fig. 14. As can be seen in Fig. 14, it is observed that there are generally no visible cracks on the inner surface of the HSSCC series, pores are formed in very low amounts, and the transitions between aggregate and cement paste are quite void-free.

Mathematical correlation can be used to predict the hardened properties of the HSSCC series based on the data obtained. In general, an R^2 value above 0.7 indicates a strong correlation between properties [81,82]. Fig. 15 shows the relationships and equations between the flexural and compressive strength results obtained from the 28 and 90-day HSSCC series. As seen in Fig. 15, it was determined that the compressive strength values increased with the increase in flexural strength values, and there was a positive and strong compatibility relationship between the strengths.

3.2.4. *Apparent porosity test results*

The variation of apparent porosity values of the HSSCC series according to curing times is given in Fig. 16. As can be seen in Fig. 16, the apparent porosity values in all series decreased with increasing curing time. The apparent porosity values of the HSSCC series after 28 days of curing ranged between 4.9 and 7.1%, after 56 days of curing between 3.1 and 4.3% and after 90 days of curing between 1.7 and 2.4%.

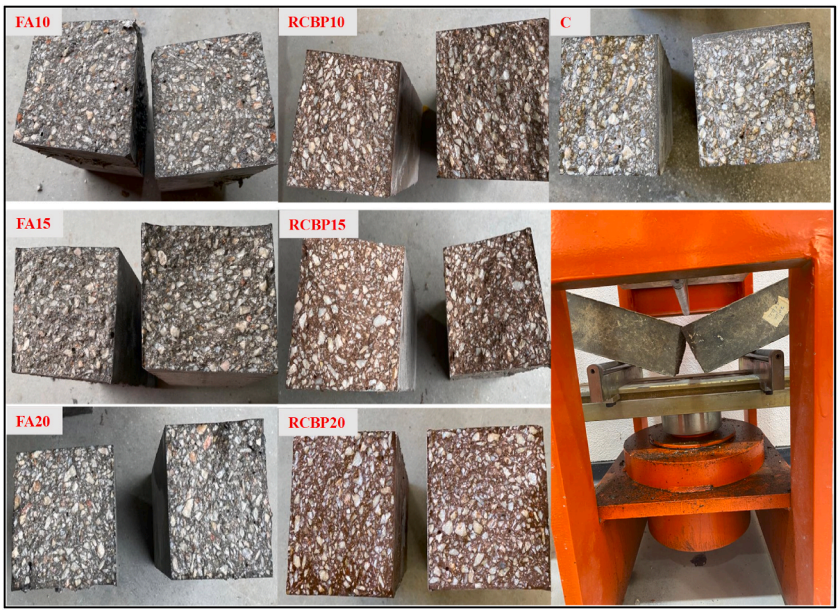

Fig. 14. Cross-sectional views of HSSCC series (90 days) after fracture under flexural strength test.

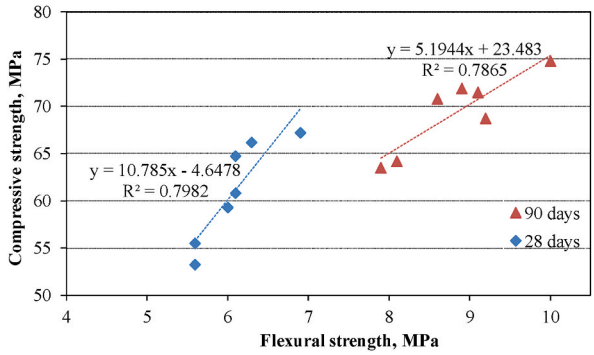

Fig. 15. Relationships between 28 and 90 day flexural and compressive strengths of HSSCC series.

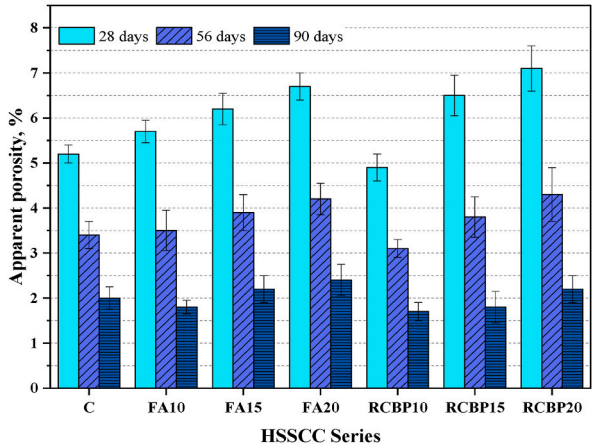

Fig. 16. Apparent porosity measurement results of HSSCC series according to curing times.

The apparent porosity values of the C series at the end of 28, 56 and 90 days of curing were 5.2%, 3.4% and 2%, respectively. When Fig. 16 is examined; The apparent porosity values of the FA10, FA15 and FA20 series at the end of the 28th day are respectively compared to the C series; While it increased by 9.6%, 19.2% and 28.8%, it decreased by 5.8% in RCBP10 and increased by 25% and 36.5% in the RCBP15 and RCBP20 series, respectively. The apparent porosity values of the FA series at the end of the 56th day increased by 2.9%, 14.7% and 23.5% in the FA10, FA15 and FA20 series, respectively, while in the RCBP series; it decreased by 8.8% in the RCBP10, increased by 11.8% and 26.5% in RCBP15 and RCBP20 series, respectively. Thus, at the end of the 56th day, it was determined that the apparent porosity values of the other series increased with the increase of FA and RCBP replacement in the HSSCC series, except the RCBP10 series. When the apparent porosity values at the end of the 90-day cure were analyzed according to the C series, there was a 10% decrease in the FA10 series, while the porosity values of the FA15 and FA20 series increased by 10% and 20%, respectively. In the RCBP series, the RCBP10 and RCBP15 series decreased by 15% and 10%, respectively, while the RCBP20 series

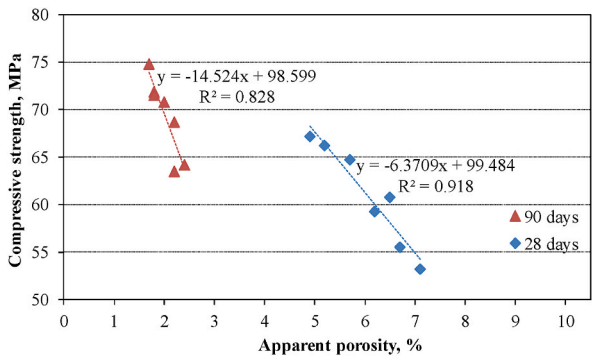

Fig. 17. Relationships between 28 and 90 day apparent porosity values and compressive strengths of HSSCC series.

increased by 10%. Thus, it was determined that the FA10, RCBP10 and RCBP15 series reached lower apparent porosity values than series C at the end of the 90th day. When the apparent porosities of the HSSCC series were analyzed in general, the differences between the FA and RCBP substituted series and the C series were higher in the first 28 days and gradually decreased at the end of the 90th day. This can be explained by the fact that FA and RCBP filled the pores of HSSCC after their pozzolanic activities, causing the development of new products and decreasing the porosity of the concrete over time. In addition, the higher fineness of RCBP compared to cement may also have contributed to filling the micropores of the mortars. Similar results were also found by other researchers [49].

Fig. 17 shows the relationship and equations between 28 and 90 days of apparent porosity values and compressive strengths of the HSSCC series. As seen in Fig. 17, compressive strengths decrease with increasing apparent porosity values, and there is a strong and negative relationship between them.

3.2.5. Water absorption test results

Water absorption is directly related to the durability or long-term behavior of concrete. The presence of pores and cracks in concrete increases the absorption of water in concrete, which consequently affects its mechanical and other durability properties [5, 83]. Fig. 18 presents the results of the water absorption by weight test, showing the effect of replacing FA and RCBP with cement on the water absorption properties of HSSCC.

Water absorption values for all HSSCC series were 1.9–2.8% on day 28 and 0.9–1.35% on day 90. The water absorption values of series C after 28, 56 and 90 days of curing are 2.1%, 1.5% and 1.1%, respectively. Since water absorption has a direct relationship with voids, water absorption decreased over time as the voids decreased with increasing curing time and the internal structure was improved. This improvement in water absorption resistance can be attributed to a denser concrete matrix [84]. In general, the results of water absorption tests show a direct proportional relationship with the amount of FA in HSSCC; that is, as the content increases, the water absorption rate increases [5]. When Fig. 18 is analyzed, the water absorption values of FA10, FA15 and FA20 series at the end of the 28th day increased by 4.8%, 14.3% and 23.8%, respectively, while it decreased by 9.5% in RCBP10 and increased by 19% and 33.3% in RCBP15 and RCBP20 series, respectively, compared to C series. At the end of the 56th day, the water absorption values of the FA series decreased by 6.7% in FA10 and increased by 13.3% and 20% in the FA15 and FA20 series, respectively, compared to the C series. In the RCBP series, while it decreased by 10% in RCBP10, it increased by 6.7% and 26.7% in RCBP15 and RCBP20 series. Thus, at the end of the 56th day, it was determined that with the increase of FA and RCBP replacement in the HSSCC series, the water absorption values of the other series increased except for the FA10 and RCBP10 series. When the water absorption values at the end of 90 days of cure were analyzed according to the C series, the FA10 series decreased by 13.6%, while the water absorption values of the FA15 and FA20 series increased by 9.1% and 18.2%, respectively. In the RCBP series, the RCBP10 and RCBP15 series decreased by 18.2% and 4.5%, respectively, while the RCBP20 series increased by 22.7%. When the water absorption values of the HSSCC series up to 90 days are analyzed in general, it is found that the differences between the FA and RCBP substituted series and the C series are higher in the first 28 days and gradually decrease at the end of the 90th day, similar to the apparent porosity measurements.

Low water absorption is an indication of good compaction provided by the concrete's own weight. Better compaction can be expected, especially in the presence of FA, due to increased workability. The appearance of pores, defects and cracks in concrete increases the water absorption rate of concrete, which in turn affects the mechanical properties and other durability characteristics [74]. It has been noticed that increasing FA replacement in HSSCC increases water absorption at an earlier age. This is because increasing the amount of class F FA in concrete reduces the hydration process at earlier ages. At earlier ages, the hydration process in concrete with high FA content is not complete and permeable capillary pores are still present. This can lead to higher water absorption [73]. The water absorption values at day 90 of the HSSCC series decreased by 48%, 57%, 50% and 51% for C, FA10, FA15 and FA20, respectively, and by 53%, 58% and 52% for RCBP10, RCBP15 and RCBP20, respectively, compared to day 28. The porosity amounts of FA10, RCBP10 and RCBP15 series decreased generally more than the other series from 28 days to 90 days. The water absorption results of FA-replacement concrete in the study by Ting et al. [73] changed similarly. The decrease in water absorption of HSSCCs with RCBP

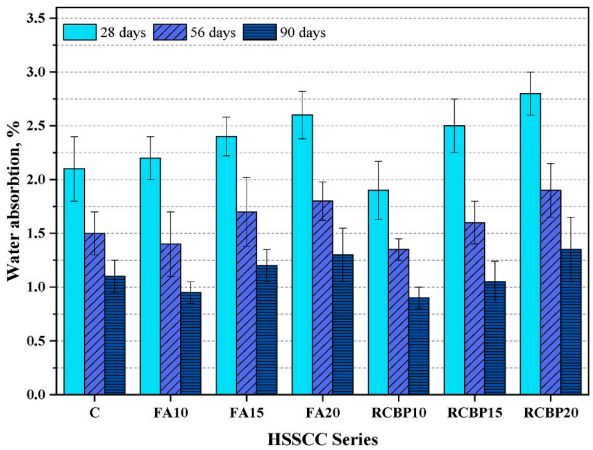

Fig. 18. Water absorption measurement results of HSSCC series according to curing times.

replacement in RCBP10 and RCBP15 could clearly be due to pozzolanic reactivity, as suggested in previous studies [49,85].

The relationships between 28 and 90 days of water absorption and compressive strength for the HSSCC series are given in Fig. 19. As expected, higher water absorption corresponds to lower compressive strength, and there is a strong relationship between them.

3.2.6. Statistical evaluations

In order to increase the accuracy of performance prediction methods for HSSCC design, it is generally necessary to increase the amount of experiments to be performed. This may lead to increased costs and additional time. In this context, it is useful to perform sensitivity analyses to determine which parameters affect which properties in HSSCC designs in order to facilitate future studies. Sensitivity analysis helps to explain the effect of variables on the predicted properties. Sensitivity analysis using regression techniques is a method for evaluating how variables affect the outcome of a statistical model.

In some studies [86–88] in the literatüre statistically significant parameters were obtained from SCC design variables. The experimental findings obtained from this study were statistically analyzed using linear analysis and Pearson correlation matrix.

HSSCC is a mixture of various material components precisely proportioned according to certain standards. The small number of concrete designs and specimens produced in the studies to be carried out may cause inadequate statistical evaluation and prediction models. In this study, slump-flow, V-funnel flow and L-box height ratio values, which are compressive strength, flexural strength and workability properties, were selected as dependent variables. From the linear regression analysis (LRA), it was found that the fresh and mechanical properties of HSSCC did not depend on any independent variable only. The utilization rate (%) of RCBP and FA used as cement replacements in the HSSCC design, the amount of HRWRA (%) and the curing time were determined as independent variables. The analyses were carried out at 5% significance level and the degree of influence of the dependent parameters on the independent parameters and their relationships were determined.

Multiple linear model analysis was used to determine the effects of the design parameters used in the mixture on the experimental results applied to the HSSCC series. The results of the analyses are shown in Table 4. The formulae of the multiple regression equations obtained in the analyses are given in equations (5)–(9) below.

$$CS = 64.088 + (-0.544)*FA\% + (-0.496)*RCBP\% + (0.134)*T \quad (5)$$

$$FS = 5.342 + (-0.045)*FA\% + (-0.035)*RCBP\% + (0.044)*T \quad (6)$$

$$SF = 193.571 + (4.057)*FA\% + (-5.000)*RCBP\% + (282.381)*HRWRA \quad (7)$$

$$VF = 30.107 + (-0.194)*FA\% + (0.150)*RCBP\% + (-8.845)*HRWRA \quad (8)$$

$$L_{box} = 0.356 + (0.004)*FA\% + (-0.005)*RCBP\% + (0.276)*HRWRA \quad (9)$$

CS: Compressive strength (MPa), FS: Flexural strength (MPa), SF: Slump-flow diameter (mm), VF: V-funnel flow time (sec), L_{box}=L-box height ratio, RCBP%: RCBP replacement level (%), FA%: FA replacement level (%), HRWRA%: HRWRA level (%), T: Curing time (day).

The equations presented above were used to predict the CS, FS, SF, VF and L_{box} results of the HSSCC series produced in the present research. The relationships between the experimental results obtained from the HSSCC series and the prediction results are shown in Fig. 20 below.

The results of the statistical evaluation (Table 4) showed that RCBP replacement level (%), FA replacement level (%) and curing time had a statistically significant effect on the compressive and flexural strengths of HSSCC. Among the design parameters, curing time (T) had the highest effect on CS and FS with 38.4% and 86.3%, respectively, while FA replacement level (%) had the lowest effect on CS and FS with 21% and 2.8%, respectively. However, RCBP replacement level (%) was the parameter with an effect of 37.9% for CS.

The correlation matrices created to show the relationship and degree of correlation between design parameters and experimental results are presented in Figs. 21 and 22. Figs. 21 and 22 show the Pearson correlation matrices of the machinability and mechanical test results of the design parameters, respectively. The correlation matrices show the degree of correlation between each parameter. In general, an absolute correlation coefficient above 0.8 between two properties indicates a high degree of linear relationship [89]. Accordingly, when the coefficients between 0.6 and 0.8 are considered as "good" and 0.8–1.0 as "high" levels of correlation, the following evaluations were made.

RCBP replacement level (%): a negative relationship with slump-flow and L-box height ratio with a high correlation coefficient; a positive relationship with V-funnel flow time with a good correlation coefficient.

FA replacement level (%): a positive relationship with slump-flow and L-box height ratio with a high correlation coefficient; a negative relationship with V-funnel flow time with a high correlation coefficient.

HRWRA level (%): a negative relationship with slump-flow and L-box height ratio with a good correlation coefficient; a positive relationship with V-funnel flow time with a good correlation coefficient.

Curing time (T): a positive relationship with flexural strength with a high correlation coefficient; a positive relationship correlation with compressive strength with a good correlation coefficient.

3.2.7. Internal structure analysis

Microstructural analysis of the HSSCC series has a significant impact on the evaluation of the properties of concrete components, such as strength and durability. Internal structure analysis by SEM is useful to better understand the performance of concrete and the

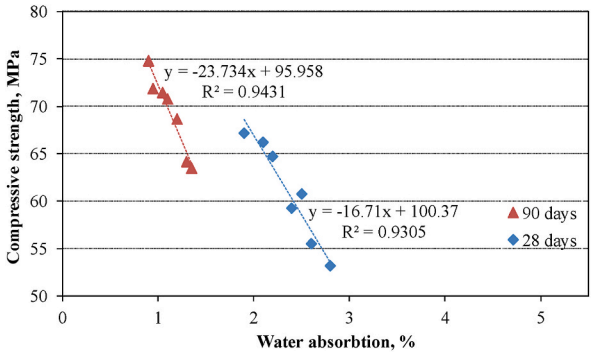

Fig. 19. Relationships between 28 and 90 day water absorption values and compressive strengths of HSSCC series.

Table 4
Statistical analysis of strength test results.

Dependent variable	Independent variable	Statistical parameters				
		Sequential sum of squares	Mean square	Computed F	P-value	Contribution
Compressive strength	RCBP replacement level (%)	240.849	80.283	55.974	0.000	37.9%
	FA replacement level (%)	133.342	44.447	30.989	0.000	21%
	Curing time, (day)	244.475	122.238	85.225	0.000	38.4%
	Error	17.211	1.434	–	–	2.7%
	Total	635.878	–	–	–	–
Flexural strength	RCBP replacement level (%)	2.920	0.973	12.735	0.005	9.5%
	FA replacement level (%)	0.850	0.283	3.707	0.081	2.8%
	Curing time, (day)	26.606	26.606	348.121	0.000	86.3%
	Error	0.459	0.076	–	–	1.4%
	Total	30.835	–	–	–	–

surface morphology of cement paste.

SEM (x3000 magnification) and Energy Dispersive X-ray (EDX) analyses of the C series samples at 28 and 90 days are shown in Fig. 23. As seen in Fig. 23 a, the amount of microcracks observed at early ages (28 days) decreased as the curing time progressed (90 days). Series C reached a more compact internal structure after 90 days of curing. Thus, the amount of C-S-H and C-H structures obtained as a result of hydration reactions increased. The probability of large voids during mixing and placement in HSSCC production is much lower than in conventional vibrated concrete. As can be seen in Fig. 23, no large voids were observed in the C series. The interfacial transition zone (ITZ) between cement paste and aggregate is one of the important factors affecting the mechanical properties of concrete. As the curing period increased from 28 days to 90 days, hydration progressed, microcracks decreased, the porosity of the ITZ decreased, and its thickness decreased. This was considered to contribute to the improvement of compressive and flexural strengths by creating a strong bond between aggregate and cement paste.

As the curing age of the HSSCC series increased, the hydration process in the matrix progressed, and dense hydration products and a few pores were formed. From EDX analysis, at early curing ages (28 days), the structure containing less calcium (Ca) can be seen, while at later ages (90 days), the presence of silica (Si) reached a noticeable level. EDX analysis includes mainly Ca, Si and Al spectra, along with other elements. Since about half of the EDX line is located above the aggregate surface, ITZs were detected and approximately marked on the SEM images.

SEM (x3000 magnification) images of HSSCC specimens with FA and RCBP series at 28 and 90 days are shown in Figs. 24 and 25. As shown in Figs. 24 and 25, the amount of visible voids and microcracks in the internal structure of the series increased as the FA and RCBP replacement ratios in the HSSCC mixtures increased and decreased as the curing time increased. Microcracks in concrete are especially prevalent in ITZs. This is mainly due to poor hydration process and insufficient gel formation between cement paste and aggregate [90].

From the SEM analysis, it is observed that the internal structure of the FA10 series is more compact and compliant in all regions than the other FA-substituted series. This can be interpreted as a strong bond between the aggregate grains and the binder phase pulp of the FA10 series. From the SEM images (Fig. 24c and 24f) of the 28 and 90-day samples of the FA20 series, which has the highest FA replacement, it is determined that the amount of unreacted (spherical and smooth) or partially reacted FA particles is high, and the number and width of microcracks are higher than the other FA series. In addition, it was found that the number of unreacted or partially reacted FA particles observed in 28-day SEM images of FA series decreased at the end of 90 days, and coating layers (CSHs) were formed on them with the effect of pozzolanic reaction [91,92]. The inadequate reaction of FA at 28 days may also be a reason for the decrease in the compressive strength of the mixture with the addition of high amounts of FA to HSSCC [71]. Furthermore, as seen in Fig. 24e and 24 f, FA is found to contain a significant proportion of particles with hollow spheres. When these hollow spherical particles are partially dissolved, they can form highly dispersed small-sized pores. However, the SEM images (Fig. 24b and 24 c) also show the

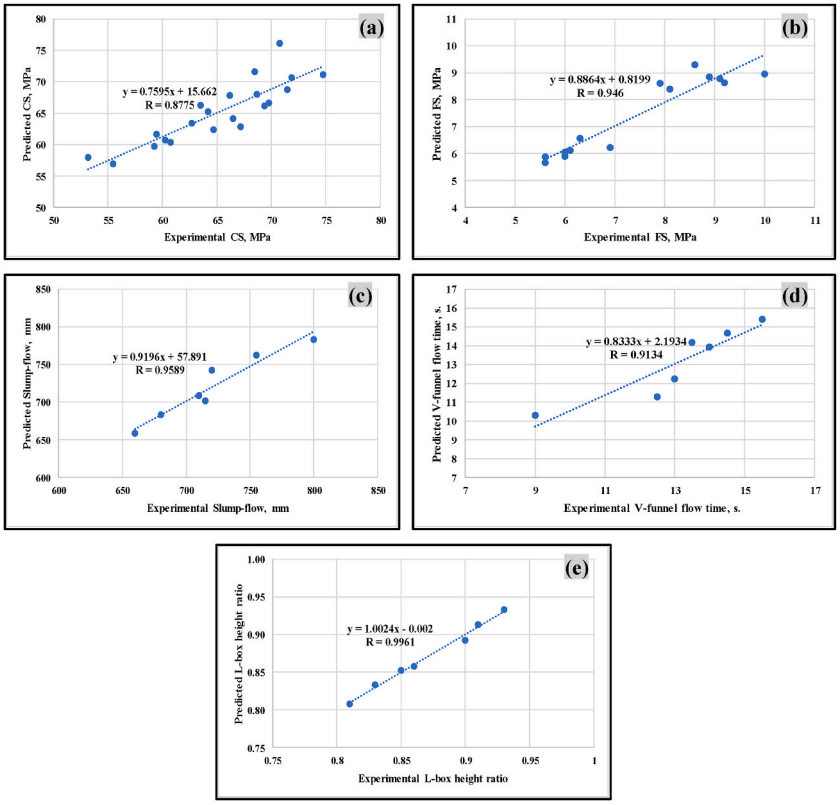

Fig. 20. Relationships between prediction and experimental results of HSSCC series; (a) CS, (b) FS, (c) Slump-flow, (d) V-funnel, (e) L_{box}.

(a)

SF	1			
FA%	0.895	1		
RCBP%	-0.800	-0.664	1	
HRWRA%	-0.738	-0.706	0.941	1
	SF	FA%	RCBP%	HRWRA%

(b)

VF	1			
FA%	-0.885	1		
RCBP%	0.717	-0.664	1	
HRWRA%	0.687	-0.706	0.941	1
	VF	FA%	RCBP%	HRWRA%

(c)

L-box	1			
FA%	0.926	1		
RCBP%	-0.838	-0.664	1	
HRWRA%	-0.773	-0.706	0.941	1
	L-box	FA%	RCBP%	HRWRA%

Fig. 21. Pearson correlation matrices of the determined design parameters and HSSCC series machinability test results; (a) SF, (b) VF, (c) L-box.

(a)

CS	1			
FA%	-0.307	1		
RCBP%	-0.194	-0.664	1	
T	0.619	0.000	0.000	1
	CS	FA%	RCBP%	T

(b)

FS	1			
FA%	-0.113	1		
RCBP%	-0.031	-0.664	1	
T	0.929	0.000	0.000	1
	FS	FA%	RCBP%	T

Fig. 22. Pearson correlation matrices of the determined design parameters and HSSCC series mechanical test results; (a) CS, (b) FS.

increasing width of the ITZ, which can be considered as the reason for the decrease in strength as well as higher water absorption and increased amount of porosity. The high workability resulting from the replacement of FA in HSSCC increases the homogeneity of the hardened concrete. This can be considered as contributing to the increase in flexural strength of FA10 and FA15 by strengthening the interlocking bond between cement paste and aggregates. In addition, observed in the SEM images of the FA-replacement series (Fig. 24), FA particles, which are completely unreacted and spherical in shape, fill the voids and form denser packing in the matrix

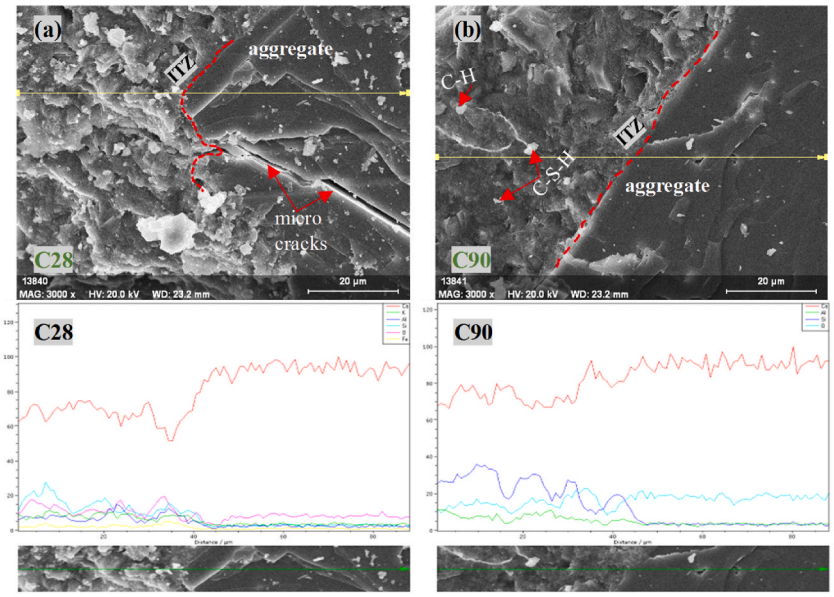

Fig. 23. SEM - EDX analysis of control (C) series; (a) 28 days, (b) 90 days.

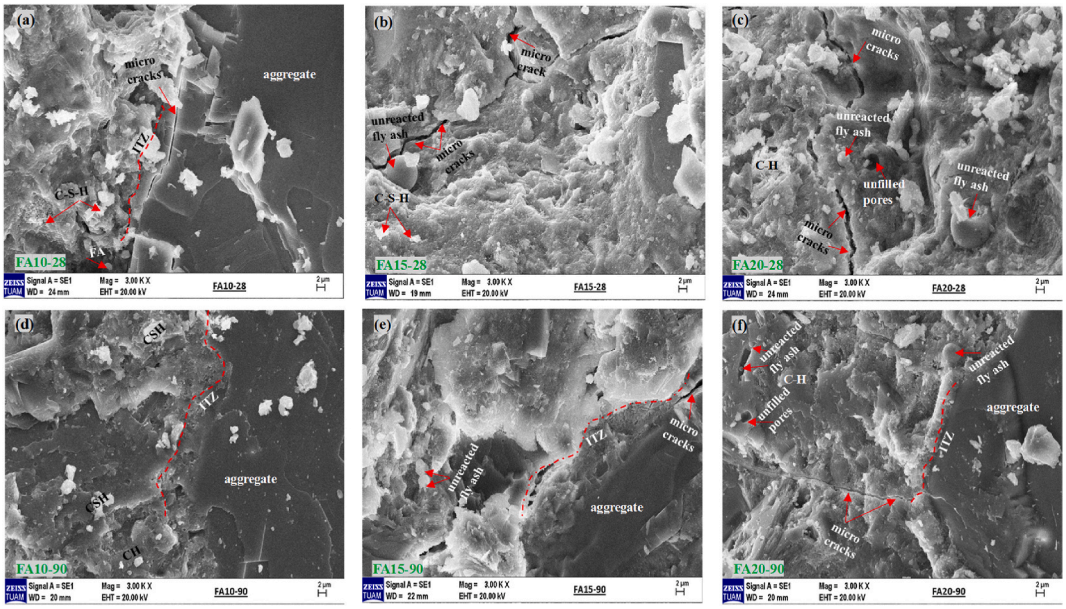

Fig. 24. SEM analyses of FA-substituted HSSCC series; (a) 28 days FA10, (b) 28 days FA15, (c) 28 days FA20, (d) 90 days FA10, (e) 90 days FA15, (f) 90 days FA20.

phase, which has been evaluated in several studies [80,92] as contributing to the strengths.

FA can eliminate the growth of calcium hydroxide or convert calcium hydroxide to C-S-H by a pozzolanic reaction. FA particles in the concrete mix react with CH over time to form C-S-H gels, and this process continues for years [93]. Furthermore, pozzolanic reactions provide HSSCC with fine pore structure, low permeability, long-term strength-gaining properties and reduction of the thickness of ITZ [80]. Thus, the bond strength between cement paste and aggregate is also increased. As shown in Fig. 24, the thickness of the ITZs in the FA series at the end of 90 days of curing became thinner and stronger compared to the 28-day series.

It was observed that the internal structure of the RCBP10 series was more compact and coherent in all regions than the other RCBP series, and the C-S-H gels formed were better distributed with strong ITZ formation (Fig. 25a, 25d). This is considered to be the reason for the higher mechanical strengths of the RCBP10 series.

SEM images at x5000 magnification and EDX analysis of C, RCBP10 and FA10 series, which reached the highest mechanical strengths among the HSSCC series, are shown in Fig. 26. At the end of 90 days, the highest amount of Si in the HSSCC series is observed

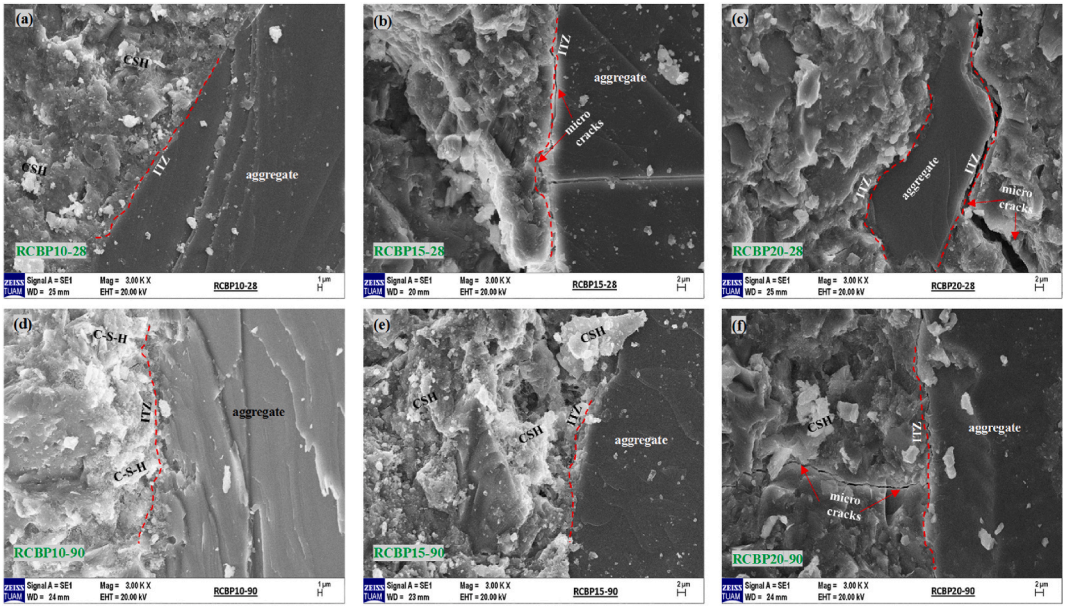

Fig. 25. SEM analyses of RCBP-substituted HSSCC series; (a) 28-day RCBP10, (b) 28-day RCBP15, (c) 28-day RCBP20, (d) 90-day RCBP10, (e) 90-day RCBP15, (f) 90-day RCBP20.

in RCBP10. The concrete matrix with 10% RCBP replacement in HSSCC contains relatively dense hydration products and the least number of pores compared to the other series, showing a denser microstructure than the internal structure of the HSSCC specimen with C series. The EDX pattern presented in Fig. 26 a shows the highest proportions of elements in the control (C) series. As is well known, EDX is used to identify the element on material surfaces and provide information on its quantitative composition. Fig. 26 a shows that the main elements in the C series are calcium, silicon and aluminum. The presence of FA in the FA10 series increased the high Si content of the mixture and led to the production of more C-S-H gels, the main product of the pozzolanic reaction. It was also observed that spherical FA particles filled the matrix pores, and C-S-H gels adhered to the FA surface, forming a relatively compact structure. EDX analysis revealed the most dominant elements. Accordingly, Ca and Si concentrations in the RCBP10 series are higher than in the C and FA10 series. The presence of more Ca and Si in the concrete matrix can be interpreted as the formation of a significant amount of C-S-H gel in the HSSCC mix [81].

4. Conclusions

The following results were obtained within the framework of the experimental and statistical works carried out to investigate the

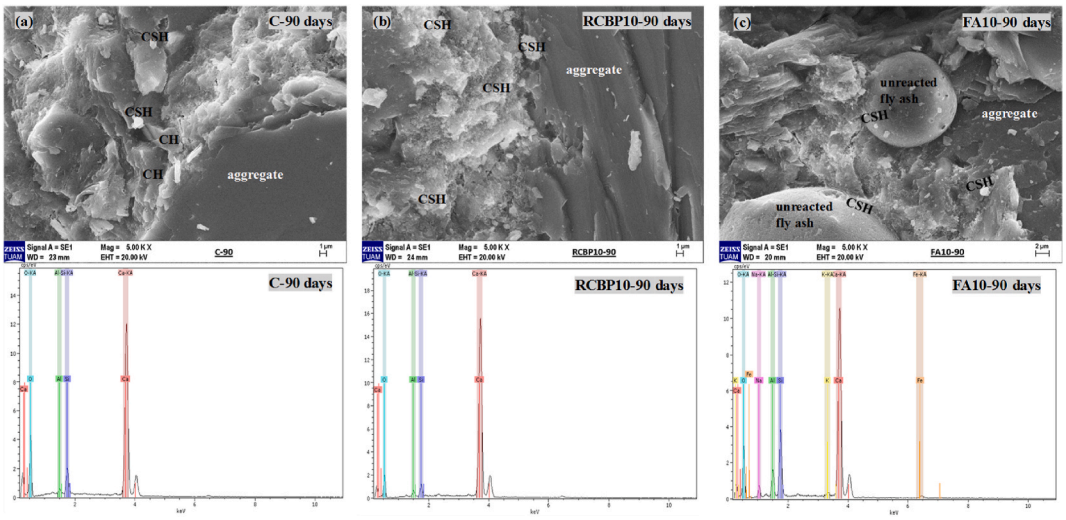

Fig. 26. SEM and EDX analyses of HSSCC series at x5000 magnification (a) 90-day C, (b) 90-day RCBP10, (c) 90-day FA10.

usability of RCBP obtained by recycling brick and tile waste in CDWs as a cement substitute in HSSCC and to compare it with the use of FA, an industrial waste. In this context;

- The highest workability values in the HSSCC series were realized in FA20 compared to the C series, while the lowest was realized in RCBP20. While FA, which is used instead of cement in HSSCC, is composed of completely spherical and smooth surface particles, which increased the workability, the irregular, rough structure of RCBP and its higher specific surface area than cement decreased the workability.
- Among the HSSCC series, the compressive strengths of FA15, FA20 and RCBP20 series were below series C at all curing times. This was attributed to the decrease in the amount of C-S-H gels and C-H due to the decrease in the cement content in the mixture and the low bonding between aggregate and paste, as observed from SEM analysis.
- After 90 days of curing, the compressive strengths of RCBP10 and RCBP15 increased by 5.6% and 1%, respectively, compared to the C series. This is due to the micro-filling ability of the substituted RCBP and the formation of better hydration products, which were detected in SEM and EDX analyses.
- In general, the increase in FA and RCBP used in the HSSCC series decreased the 28-day compressive strengths (except RCBP10), while the strength losses gradually decreased as the curing age increased and at the end of 90 days; the compressive strengths of FA10, RCBP10 and RCBP15 series were obtained above the C series.
- Similar to the compressive strengths, the flexural strengths of the HSSCC series at the end of the first 28 days decreased in all series except RCBP10. After 90 days of curing, the flexural strengths of RCBP10 and RCBP15 increased by 16.3% and 5.8%, and FA10 and FA15 increased by 3.5% and 7%, respectively.
- The apparent porosity of the HSSCC series decreased with increasing curing time and ranged between 1.7 and 2.4% at the end of 90 days. At the end of 90 days of curing, the apparent porosity and water absorption values of the FA10, RCBP10 and RCBP15 series, which had the highest mechanical strength values, also reached lower values than the C series.
- The results of the statistical evaluation showed that RCBP replacement ratio (%), FA replacement ratio (%) and curing time had a significant effect on the compressive strength of HSSCC by 37.9%, 21% and 38.4%, respectively.
- From SEM analysis, it was determined that hydration in series C progressed, microcracks decreased, and ITZ porosity decreased with the increase in curing time from 28 days to 90 days. The number of visible voids and microcracks formed in the internal structure of the series increased as the FA or RCBP replacement rates in HSSCC mixtures increased and decreased as the curing time increased. However, it was observed that HSSCC matrices with 10% FA or RCBP replacement contained more dense hydration products and fewer pores than the other series at the end of 90 days.

CRediT authorship contribution statement

Ahmet Ferdi Şenol: Writing – review & editing, Writing – original draft, Visualization, Validation, Supervision, Methodology, Investigation, Formal analysis, Data curation, Conceptualization. **Cenk Karakurt:** Writing – review & editing, Validation, Supervision, Methodology.

Declaration of competing interest

The authors declare that they have no known competing financial interests or personal relationships that could have appeared to influence the work reported in this paper.

Data availability

Data will be made available on request.

References

[1] S.K. Mezzal, Z. Al-Azzawi, K.B. Najim, Effect of discarded steel fibers on impact resistance, flexural toughness and fracture energy of high-strength self-compacting concrete exposed to elevated temperatures, Fire Saf. J. 121 (May 2021) 103271, https://doi.org/10.1016/J.FIRESAF.2020.103271.
[2] H. Okamura ve, M. Ouchi, Self-compacting concrete, J. Adv. Concr. Technol. (2003) 5–15.
[3] A. Raif Boğa, C. Karakurt, A. Ferdi Şenol, The effect of elevated temperature on the properties of SCC's produced with different types of fibers, Construct. Build. Mater. 340 (Jul 2022) 127803, https://doi.org/10.1016/J.CONBUILDMAT.2022.127803.
[4] J. Liu, S. Zang, F. Yang, R. Hai, Y. Yan, Fracture properties of steel fibre reinforced high-volume fly ash self-compacting concrete, Case Stud. Constr. Mater. 18 (Jul 2023) e02110, https://doi.org/10.1016/J.CSCM.2023.E02110.
[5] N. Singh, P. Kumar, P. Goyal, Reviewing the behaviour of high volume fly ash based self compacting concrete, J. Build. Eng. 26 (Nov 2019) 100882, https://doi.org/10.1016/J.JOBE.2019.100882.
[6] W. Shen, et al., Experimental investigation on the high-volume fly ash ecological self-compacting concrete, J. Build. Eng. 60 (Nov 2022) 105163, https://doi.org/10.1016/J.JOBE.2022.105163.
[7] EFNARC, The European Guidelines for Self-Compacting Concrete: Specification, 27, May 2005, pp. 1–68.
[8] Turkish Standards Institute, TS 802, Design of concrete mixes. Ankara, Turkiye (2016).
[9] A. Raif Boğa, A. Ferdi Şenol, The effect of waste marble and basalt aggregates on the fresh and hardened properties of high strength self-compacting concrete, Construct. Build. Mater. 363 (Jan 2023) 129715, https://doi.org/10.1016/J.CONBUILDMAT.2022.129715.
[10] B. Sukumar, K. Nagamani, R. Srinivasa Raghavan, Evaluation of strength at early ages of self-compacting concrete with high volume fly ash, Construct. Build. Mater. 22 (7) (Jul 2008) 1394–1401, https://doi.org/10.1016/J.CONBUILDMAT.2007.04.005.
[11] A. Jain, R. Gupta, S. Chaudhary, Sustainable development of self-compacting concrete by using granite waste and fly ash, Construct. Build. Mater. 262 (Nov 2020) 120516, https://doi.org/10.1016/J.CONBUILDMAT.2020.120516.

[12] R. Choudhary, R. Gupta, R. Nagar, Impact on fresh, mechanical, and microstructural properties of high strength self-compacting concrete by marble cutting slurry waste, fly ash, and silica fume, Construct. Build. Mater. 239 (Apr 2020) 117888, https://doi.org/10.1016/J.CONBUILDMAT.2019.117888.
[13] R. Choudhary, R. Gupta, T. Alomayri, A. Jain, R. Nagar, Permeation, corrosion, and drying shrinkage assessment of self-compacting high strength concrete comprising waste marble slurry and fly ash, with silica fume, Structures 33 (Oct 2021) 971–985, https://doi.org/10.1016/J.ISTRUC.2021.05.008.
[14] R.K. Rohman, S.A. Kristiawan, H.A. Saifullah, A. Basuki, The development length of tensile reinforcement embedded in high volume fly ash-self compacting concrete (HVFA-SCC), Construct. Build. Mater. 348 (Sep 2022) 128680, https://doi.org/10.1016/J.CONBUILDMAT.2022.128680.
[15] H. Singh, R. Siddique, Utilization of crushed recycled glass and metakaolin for development of self-compacting concrete, Construct. Build. Mater. 348 (Sep 2022) 128659, https://doi.org/10.1016/J.CONBUILDMAT.2022.128659.
[16] J. Gołaszewski, B. Klemczak, M. Gołaszewska, A. Smolana, G. Cygan, The feasibility of using a high volume of non-clinker binders in self-compacting concrete related to its basic engineering properties, J. Build. Eng. 66 (May 2023) 105893, https://doi.org/10.1016/J.JOBE.2023.105893.
[17] A. Sambangi, A. Eluru, Behaviour of sustainable high strength self-compacting concrete with electrically precipitated fly Ash(EPFA) – a thermal waste, Mater. Today Proc. 65 (Jan 2022) 860–870, https://doi.org/10.1016/J.MATPR.2022.03.452.
[18] N. Karthiga @ Shenbagam, M. Arun Siddharth, V. Kannan, C. Dhanusree, Experimental investigation of self-compacting concrete (SCC) using fly ash, Mater. Today Proc. (May 2023), https://doi.org/10.1016/J.MATPR.2023.04.582.
[19] M. Azimi-Pour, H. Eskandari-Naddaf, A. Pakzad, Linear and non-linear SVM prediction for fresh properties and compressive strength of high volume fly ash self-compacting concrete, Construct. Build. Mater. 230 (Jan 2020) 117021, https://doi.org/10.1016/J.CONBUILDMAT.2019.117021.
[20] A.M. de Souza, J.M. Franco de Carvalho, C.F.R. Santos, F.A. Ferreira, L.G. Pedroti, R.A.F. Peixoto, On the strategies to improve the eco-efficiency of self-compacting concrete using industrial waste: an analytical review, Construct. Build. Mater. 347 (Sep 2022) 128634, https://doi.org/10.1016/J.CONBUILDMAT.2022.128634.
[21] R. Siddique, Properties of self-compacting concrete containing class F fly ash, Mater. Des. 32 (3) (Mar 2011) 1501–1507, https://doi.org/10.1016/J.MATDES.2010.08.043.
[22] W. Wongkeo, P. Thongsanitgarn, A. Ngamjarurojana, A. Chaipanich, Compressive strength and chloride resistance of self-compacting concrete containing high level fly ash and silica fume, Mater. Des. 64 (Dec 2014) 261–269, https://doi.org/10.1016/J.MATDES.2014.07.042.
[23] D. Karthik, K. Nirmalkumar, R. Priyadharshini, Characteristic assessment of self-compacting concrete with supplementary cementitious materials, Construct. Build. Mater. 297 (Aug 2021) 123845, https://doi.org/10.1016/J.CONBUILDMAT.2021.123845.
[24] M. Abed, K. Rashid, M.U. Rehman, M. Ju, Performance keys on self-compacting concrete using recycled aggregate with fly ash by multi-criteria analysis, J. Clean. Prod. 378 (Dec 2022) 134398, https://doi.org/10.1016/J.JCLEPRO.2022.134398.
[25] M. Sharbaf, M. Najimi, N. Ghafoori, A comparative study of natural pozzolan and fly ash: investigation on abrasion resistance and transport properties of self-consolidating concrete, Construct. Build. Mater. 346 (Sep 2022) 128330, https://doi.org/10.1016/J.CONBUILDMAT.2022.128330.
[26] A.M. Mohammed, D.S. Asaad, A.I. Al-Hadithi, Experimental and statistical evaluation of rheological properties of self-compacting concrete containing fly ash and ground granulated blast furnace slag, Journal of King Saud University - Engineering Sciences 34 (6) (Sep 2022) 388–397, https://doi.org/10.1016/J.JKSUES.2020.12.005.
[27] P. Sahoo, A. Dwivedi, S.M. Tuppad, S. Gupta, Sequestration and utilization of carbon dioxide to improve engineering properties of cement-based construction materials with recycled brick powder: a pathway for cleaner construction, Construct. Build. Mater. 395 (Sep 2023) 132268, https://doi.org/10.1016/J.CONBUILDMAT.2023.132268.
[28] S. Gücek, K. Bekir Afacan, İ. Zorluer, The facts of Soil Amplification and Liquefaction after the earthquakes of February 6, 2023: examples of antakya, gölbaşı, türkoğlu, Afyon Kocatepe University Journal of Science and Engineering 23 (3) (2023) 740–752, https://doi.org/10.35414/akufemubid.1298648.
[29] R.A. Robayo-Salazar, J.F. Rivera, R. Mejía de Gutiérrez, Alkali-activated building materials made with recycled construction and demolition wastes, Construct. Build. Mater. 149 (Sep 2017) 130–138, https://doi.org/10.1016/J.CONBUILDMAT.2017.05.122.
[30] D. Sinkhonde, D. Mashava, Analysis of milling treatments of waste clay bricks effect on density and compressive strength of cement paste, Results in Materials 16 (Dec 2022) 100346, https://doi.org/10.1016/J.RINMA.2022.100346.
[31] H. Cheng, Reuse research progress on waste clay brick, Procedia Environ Sci 31 (Jan 2016) 218–226, https://doi.org/10.1016/J.PROENV.2016.02.029.
[32] M. Del Río Merino, P.I. Gracia, I.S.W. Azevedo, Sustainable construction: construction and demolition waste reconsidered, Waste Manag. Res. 28 (2) (2010), https://doi.org/10.1177/0734242X09103841.
[33] G. Chen, S. Li, Y. Zhao, Z. Xu, X. Luo, J. Gao, Hydration and microstructure evolution of a novel low-carbon concrete containing recycled clay brick powder and ground granulated blast furnace slag, Construct. Build. Mater. 386 (Jul 2023) 131596, https://doi.org/10.1016/J.CONBUILDMAT.2023.131596.
[34] T. Yılmaz, B. Ercikdi, H. Deveci, Utilisation of construction and demolition waste as cemented paste backfill material for underground mine openings, J. Environ. Manag. 222 (Sep 2018) 250–259, https://doi.org/10.1016/J.JENVMAN.2018.05.075.
[35] Z. He, et al., Research progress on recycled clay brick waste as an alternative to cement for sustainable construction materials, Construct. Build. Mater. 274 (Mar 2021) 122113, https://doi.org/10.1016/J.CONBUILDMAT.2020.122113.
[36] Z. Ge, Y. Feng, H. Yuan, H. Zhang, R. Sun, Z. Wang, Durability and shrinkage performance of self-compacting concrete containing recycled fine clay brick aggregate, Construct. Build. Mater. 308 (Nov 2021) 125041, https://doi.org/10.1016/J.CONBUILDMAT.2021.125041.
[37] X. Deng, et al., Recycled mineral admixtures based on recycled clay brick, J. Build. Eng. 76 (Oct 2023) 107193, https://doi.org/10.1016/J.JOBE.2023.107193.
[38] L. Likes, A. Markandeya, M.M. Haider, D. Bollinger, J.S. McCloy, S. Nassiri, Recycled concrete and brick powders as supplements to Portland cement for more sustainable concrete, J. Clean. Prod. 364 (Sep 2022) 132651, https://doi.org/10.1016/J.JCLEPRO.2022.132651.
[39] H. Zhang, B. Zhang, L. Tang, W. Zeng, Analysis of two processing techniques applied on powders from recycling of clay bricks and concrete, in terms of efficiency, energy consumption, and cost, Construct. Build. Mater. 385 (Jul 2023) 131517, https://doi.org/10.1016/J.CONBUILDMAT.2023.131517.
[40] Y. Zhao, J. Gao, C. Liu, X. Chen, Z. Xu, The particle-size effect of waste clay brick powder on its pozzolanic activity and properties of blended cement, J. Clean. Prod. 242 (Jan 2020) 118521, https://doi.org/10.1016/J.JCLEPRO.2019.118521.
[41] M. O'Farrell, S. Wild, B.B. Sabir, Pore size distribution and compressive strength of waste clay brick mortar, Cem. Concr. Compos. 23 (1) (Feb 2001) 81–91, https://doi.org/10.1016/S0958-9465(00)00070-6.
[42] X. Luo, J. Gao, S. Li, Y. Zhao, G. Chen, C. Liu, Early age hydration and autogenous shrinkage of blended cement containing brick powder, Construct. Build. Mater. 397 (Sep 2023) 132455, https://doi.org/10.1016/J.CONBUILDMAT.2023.132455.
[43] M.M. Atyia, M.G. Mahdy, M. Abd Elrahman, Production and properties of lightweight concrete incorporating recycled waste crushed clay bricks, Construct. Build. Mater. 304 (Oct 2021) 124655, https://doi.org/10.1016/J.CONBUILDMAT.2021.124655.
[44] Z. Ge, Y. Wang, R. Sun, X. Wu, Y. Guan, Influence of ground waste clay brick on properties of fresh and hardened concrete, Construct. Build. Mater. 98 (Nov 2015) 128–136, https://doi.org/10.1016/J.CONBUILDMAT.2015.08.100.
[45] M. Heikal, K.M. Zohdy, M. Abdelkreem, Mechanical, microstructure and rheological characteristics of high performance self-compacting cement pastes and concrete containing ground clay bricks, Construct. Build. Mater. 38 (Jan 2013) 101–109, https://doi.org/10.1016/J.CONBUILDMAT.2012.07.114.
[46] R. Sun, D. Huang, Z. Ge, Y. Hu, Y. Guan, Properties of self-consolidating concrete with recycled clay-brick-powder replacing cementitious material, J Sustain Cem Based Mater 3 (3–4) (2014), https://doi.org/10.1080/21650373.2014.946542.
[47] A.A. O, Effect of clay bricks powder on the fresh and hardened properties of self-compacting concrete, Iraqi Journal of Civil Engineering 12 (2) (2018), https://doi.org/10.37650/ijce.2018.172885.
[48] I. Irki, F. Debieb, S. Ouzadid, H.L. Dilmi, C. Settari, D. Boukhelkhel, Effect of Blaine fineness of recycling brick powder replacing cementitious materials in self compacting mortar, J. Adhes. Sci. Technol. 32 (9) (2018), https://doi.org/10.1080/01694243.2017.1393202.
[49] Y.F. Silva, D.A. Lange, S. Delvasto, Effect of incorporation of masonry residue on the properties of self-compacting concretes, Construct. Build. Mater. 196 (Jan 2019) 277–283, https://doi.org/10.1016/J.CONBUILDMAT.2018.11.132.
[50] F.S. Aditto, et al., Fresh, mechanical and microstructural behaviour of high-strength self-compacting concrete using supplementary cementitious materials, Case Stud. Constr. Mater. 19 (Dec 2023) e02395, https://doi.org/10.1016/J.CSCM.2023.E02395.

[51] Turkish Standards Institute. TS EN 197-1, Cement-Stage 1: General Cements-Component, 2012. Ankara. Turkiye.
[52] Turkish Standards Institute. TS 25, Natural Pozolan (Trass) for Use in Cement and Concrete - Definitions, Requirements and Conformity Criteria, 2015. Ankara. Turkiye.
[53] Turkish Standards Institute, TS EN 933-1, Tests for Geometrical Properties of Aggregates - Part 1: Determination of Particle Size of Distribution - Sieving Method, 2012. Ankara . Turkiye.
[54] Turkish Standards Institute. TS 802, Design of Concrete Mixes, 2016. Ankara. Turkiye.
[55] Turkish Standards Institute, TS EN 12350-8, Testing Fresh Concrete - Part 8: Self-Compacting Concrete - Slump-Flow Test, 2019. Ankara. Turkiye.
[56] Turkish Standards Institute, TS EN 12350-9, Testing Fresh Concrete - Part 9: Self-Compacting Concrete - V-Funnel Test, 2011. Ankara. Turkiye.
[57] Turkish Standards Institute, TS EN 12350-10, Testing Fresh Concrete - Part 10: Self-Compacting Concrete - L-Box Test, 2011. Ankara. Turkiye.
[58] Turkish Standards Institute, TS EN 12390-1,Testing Hardened Concrete - Part 1: Shape, Dimensions and Other Requirements for Specimens and Moulds, 2021. Ankara. Turkiye.
[59] Turkish Standards Institute, TS EN 12390-2, Testing Hardened Concrete - Part 2: Making and Curing Specimens for Strength Tests, 2019. Ankara. Turkiye.
[60] Turkish Standards Institute. TS EN 772-4, Methods of Test for Masonry Units - Part 4: Determination of Real and Bulk Density and of Total and Open Porosity for Natural Stone Masonry Units, 2000. Ankara. Turkiye.
[61] ASTM International, ASTM C642-21. Standard Test Method for Density, Absorption, and Voids in Hardened Concrete, 2021.
[62] Turkish Standards Institute, TS EN 12390-3,*Testing Hardened Concrete - Part 3: Compressive Strength Of Test Specimens*, 2019. Ankara. Turkiye.
[63] Turkish Standards Institute, TS EN 12390-5 Testing Hardened Concrete - Part 5: Flexural Strength of Test Specimens, 2019. Ankara. Turkiye.
[64] F.A. Mustapha, A. Sulaiman, R.N. Mohamed, S.A. Umara, The effect of fly ash and silica fume on self-compacting high-performance concrete, Mater. Today Proc. 39 (Jan 2021) 965–969, https://doi.org/10.1016/J.MATPR.2020.04.493.
[65] M. Elsayed, B.A. Tayeh, Y.I. Abu Aisheh, N.A. El-Nasser, M.A. Elmaaty, Shear strength of eco-friendly self-compacting concrete beams containing ground granulated blast furnace slag and fly ash as cement replacement, Case Stud. Constr. Mater. 17 (Dec 2022) e01354, https://doi.org/10.1016/J.CSCM.2022.E01354.
[66] M. Liu, Self-compacting concrete with different levels of pulverized fuel ash, Construct. Build. Mater. 24 (7) (Jul 2010) 1245–1252, https://doi.org/10.1016/J.CONBUILDMAT.2009.12.012.
[67] M. Uysal, M. Sumer, Performance of self-compacting concrete containing different mineral admixtures, Construct. Build. Mater. 25 (11) (Nov 2011) 4112–4120, https://doi.org/10.1016/J.CONBUILDMAT.2011.04.032.
[68] J.M. Khatib, Performance of self-compacting concrete containing fly ash, Construct. Build. Mater. 22 (9) (Sep 2008) 1963–1971, https://doi.org/10.1016/J.CONBUILDMAT.2007.07.011.
[69] A. Schackow, D. Stringari, L. Senff, S.L. Correia, A.M. Segadães, Influence of fired clay brick waste additions on the durability of mortars, Cem. Concr. Compos. 62 (Sep 2015) 82–89, https://doi.org/10.1016/J.CEMCONCOMP.2015.04.019.
[70] Y.F. Silva, S. Delvasto, S. Izquierdo, G. Araya-Letelier, Short and long-term physical and mechanical characterization of self-compacting concrete made with masonry and concrete residue, Construct. Build. Mater. 312 (Dec 2021) 125382, https://doi.org/10.1016/J.CONBUILDMAT.2021.125382.
[71] A. Jain, R. Gupta, S. Chaudhary, Sustainable development of self-compacting concrete by using granite waste and fly ash, Construct. Build. Mater. 262 (Nov 2020) 120516, https://doi.org/10.1016/J.CONBUILDMAT.2020.120516.
[72] T. Bilir, O. Gencel, I.B. Topcu, Properties of mortars with fly ash as fine aggregate, Construct. Build. Mater. 93 (Sep 2015) 782–789, https://doi.org/10.1016/J.CONBUILDMAT.2015.05.095.
[73] T.Z.H. Ting, M.E. Rahman, H.H. Lau, Sustainable lightweight self-compacting concrete using oil palm shell and fly ash, Construct. Build. Mater. 264 (Dec 2020) 120590, https://doi.org/10.1016/J.CONBUILDMAT.2020.120590.
[74] P. Promsawat, B. Chatveera, G. Sua-iam, N. Makul, Properties of self-compacting concrete prepared with ternary Portland cement-high volume fly ash-calcium carbonate blends, Case Stud. Constr. Mater. 13 (Dec 2020) e00426, https://doi.org/10.1016/J.CSCM.2020.E00426.
[75] G.F. Huseien, A.R.M. Sam, R. Alyousef, Texture, morphology and strength performance of self-compacting alkali-activated concrete: role of fly ash as GBFS replacement, Construct. Build. Mater. 270 (Feb 2021) 121368, https://doi.org/10.1016/J.CONBUILDMAT.2020.121368.
[76] W. Wongkeo, P. Thongsanitgarn, A. Ngamjarurojana, A. Chaipanich, Compressive strength and chloride resistance of self-compacting concrete containing high level fly ash and silica fume, Mater. Des. 64 (Dec 2014) 261–269, https://doi.org/10.1016/J.MATDES.2014.07.042.
[77] M. Ebrahimi, A. Eslami, I. Hajirasouliha, M. Ramezanpour, K. Pilakoutas, Effect of ceramic waste powder as a binder replacement on the properties of cement- and lime-based mortars, Construct. Build. Mater. 379 (May 2023) 131146, https://doi.org/10.1016/J.CONBUILDMAT.2023.131146.
[78] H. Zhang, C. Zhang, B. He, S. Yi, L. Tang, Recycling fine powder collected from construction and demolition wastes as partial alternatives to cement: a comprehensive analysis on effects, mechanism, cost and CO2 emission, J. Build. Eng. 71 (Jul 2023) 106507, https://doi.org/10.1016/J.JOBE.2023.106507.
[79] C. Xue, H. Qiao, H. Cao, Q. Feng, Q. Li, Analysis on the strength of cement mortar mixed with construction waste brick powder, Adv. Civ. Eng. 2021 (2021), https://doi.org/10.1155/2021/8871280.
[80] J. Guru Jawahar, C. Sashidhar, I.V. Ramana Reddy, J. Annie Peter, Micro and macrolevel properties of fly ash blended self compacting concrete, Mater. Des. 46 (Apr 2013) 696–705, https://doi.org/10.1016/J.MATDES.2012.11.027.
[81] A. Meena, N. Singh, S.P. Singh, High-volume fly ash Self Consolidating Concrete with coal bottom ash and recycled concrete aggregates: fresh, mechanical and microstructural properties, J. Build. Eng. 63 (Jan 2023) 105447, https://doi.org/10.1016/J.JOBE.2022.105447.
[82] A. Simalti, A.P. Singh, Comparative study on performance of manufactured steel fiber and shredded tire recycled steel fiber reinforced self-consolidating concrete, Construct. Build. Mater. 266 (Jan 2021) 121102, https://doi.org/10.1016/J.CONBUILDMAT.2020.121102.
[83] A. Adesina, P. Awoyera, Overview of trends in the application of waste materials in self-compacting concrete production, SN Appl. Sci. 1 (9) (2019), https://doi.org/10.1007/s42452-019-1012-4.
[84] G. Sua-iam, S. Jamnam, Influence of calcium carbonate on green self-compacting concrete incorporating porcelain tile waste as coarse aggregate replacement, Case Stud. Constr. Mater. 19 (Dec 2023) e02366, https://doi.org/10.1016/J.CSCM.2023.E02366.
[85] H. Singh, R. Siddique, Long term durability assessment of self-compacting concrete made with crushed recycled glass and metakaolin, Construct. Build. Mater. 400 (Oct 2023) 132656, https://doi.org/10.1016/J.CONBUILDMAT.2023.132656.
[86] T.T. Nguyen, H. Pham Duy, T. Pham Thanh, H.H. Vu, Compressive strength evaluation of fiber-reinforced high-strength self-compacting concrete with artificial intelligence, Adv. Civ. Eng. 2020 (2020), https://doi.org/10.1155/2020/3012139.
[87] G.S. Jameel, S. İpek, A.D. Ahmed, E. Güneyisi, E.M. Güneyisi, Rheological behavior and key properties of metakaolin and nano-SiO2 blended fibrous self-compacting concretes, Construct. Build. Mater. 368 (Mar 2023) 130372, https://doi.org/10.1016/J.CONBUILDMAT.2023.130372.
[88] G.S. Jameel, S. İpek, E. Güneyisi, E.M. Güneyisi, A.D. Ahmed, Analyzing the load-displacement behavior and determining fracture parameters and bond strength of high-strength nonfibrous and fibrous SCC mixtures, J. Build. Eng. 85 (May 2024) 108744, https://doi.org/10.1016/J.JOBE.2024.108744.
[89] E. Golafshani, N. Khodadadi, T. Ngo, A. Nanni, A. Behnood, Modelling the compressive strength of geopolymer recycled aggregate concrete using ensemble machine learning, Adv. Eng. Software 191 (May 2024) 103611, https://doi.org/10.1016/J.ADVENGSOFT.2024.103611.
[90] R. Mohana, K. Bavithra, Influence of nano materials on the macro and micro structural behaviour of high performance concrete using interfacial transition zone approach, Construct. Build. Mater. 397 (2023), https://doi.org/10.1016/j.conbuildmat.2023.132465.
[91] G. Sua-iam, N. Makul, Recycling prestressed concrete pile waste to produce green self-compacting concrete, J. Mater. Res. Technol. 24 (May 2023) 4587–4600, https://doi.org/10.1016/J.JMRT.2023.04.101.
[92] P. Chindaprasirt, C. Jaturapitakkul, T. Sinsiri, Effect of fly ash fineness on microstructure of blended cement paste, Construct. Build. Mater. 21 (7) (Jul 2007) 1534–1541, https://doi.org/10.1016/J.CONBUILDMAT.2005.12.024.
[93] S. Wang, L. Baxter, F. Fonseca, Biomass fly ash in concrete: SEM, EDX and ESEM analysis, Fuel 87 (3) (Mar 2008) 372–379, https://doi.org/10.1016/J.FUEL.2007.05.024.